Master's Thesis 2013

Candidate: Sithara Dayarathna

Title: Simulation of Gas and Liquid Flow in a Biogas Reactor Using Fluent

Telemark University College
Faculty of Technology
Kjølnes
3914 Porsgrunn
Norway

Telemark University College
Faculty of Technology
M.Sc. Programme

MASTER'S THESIS, COURSE CODE FMH606

Student:	**Sithara Dayarathna**
Thesis title:	**Simulation of gas and liquid flow in a biogas reactor using Fluent**
Signature:	. . . . .
Number of pages:	79
Keywords:	**Biogas reactor, CFD simulation, GAMBIT, FLUENT, Euler-Euler approach, Gas liquid flow characteristics, Boundary conditions, Bubble size, Velocity vectors, Liquid recirculation**

Supervisor:	Knut Vågsæther	sign.:	. . . . .
2nd Supervisor:	<name>	sign.:	. . . . .
Censor:	<name>	sign.:	. . . . .
External partner:	VEAS	sign.:	. . . . .
Availability:	Open		

Archive approval (supervisor signature)**:** sign.: . . . . . **Date :** . . . . . .

Abstract:

Anaerobic Digestion (AD) is a popular secondary treatment method to handle biological wastes in sewage and wastewater treatment plants due to its multiple benefits apart from the waste reduction. One of the biogas reactors at VEAS, a large scale sewage treatment plant located at Oslo area has been focused on this study. CFD simulations have been used to simulate the gas and liquid flow fields in the reactor in order to investigate the influence of certain boundary conditions and others factors on the gas and liquid flow characteristics and to provide recommendation to improve the performance of the reactor.

Commercial CFD software, ANSYS FLUENT 13.0 has been used for the simulations and GAMBIT 2.4.6 version, a preprocessor to FLUENT has been used to generate the problem geometry and computational mesh. Euler-Euler approach was used as the general multiphase model and liquid and biogas phases were assumed as water and air respectively. Transient simulations were performed with different gas bubble sizes of 1 mm, 5 mm and 10 mm, different inlet velocities of 1.2 m/s and 0.6 m/s and with the presence of a source term for the gas phase. In addition, the existing gas distribution arrangement at the VEAS was also simulated to compare the gas and liquid flow characteristics.

The results from the simulation demonstrated a similar flow pattern for 5 mm and 10 mm bubble sizes. Considering the stability of the system, the 10 mm bubble size showed a faster convergence at each time step than the other cases and achieved rather stable flow pattern in a shorter period of time. The low inlet gas velocity case of 0.6 m/s showed a poor liquid velocity distribution compared to that of 1.2 m/s inlet gas velocity case. Inclusion of the source term does not reflect any significant change in the liquid flow fields.

The existing gas distribution arrangement at VEAS which uses only 5 pipes at a time showed a different liquid and gas velocity profiles and liquid recirculation patterns. A bulk liquid motion towards the gas inlets were identified in this arrangement while the initial gas distribution arrangement displayed a much better recirculation of liquid throughout the whole liquid volume.

Table of Contents

Preface

This study has been carried out as an initial phase of a research project between Telemark University College and VEAS sewage tratement plant at Røyken. This report will provide a basic overview to the simulation of gas and liquid flow in one of the biogas reactors at VEAS and briefly discuss the influence of certain boundary conditions on the flow characteristics and performances of the reactors.

I would like to express my sincere grattude to my supervisor, Associate Professor Knut Vågsæther for his continuous guidance and support throughout the entire time period of this thesis. I would also like to thank the external partner of this thesis, VEAS for providing with the necessary information of the biogas reactors.

Finally, I am also thankful to Christian Lunden at IT support center of Telemark University College and my friend Chameera Jayarathna for extending their fullest support during this work.

Porsgunn, June 1, 2013

Sithara Dayarathna

Abbreviations

AD	Anaerobic digestion/Anaerobic digester
CFD	Computational fluid dynamics
CH_4	Methane
CO_2	Carbon dioxide
CO	Carbon monoxide
CPU	Central processing unit
CSTR	Continuous stirred tank reactors
DS	Dissolved solids
EGSB	Expanded granular sludge beds
ELALR	External air lifts reactors
GHG	Greenhouse gas
H_2	Hydrogen
H_2S	Hydrogen sulphide
ILALR	Internal air lift reactors
N_2	Nitrogen
NH_3	Ammonia
N_2O	Nitrous oxide
O_2	Oxygen
TSS	Total suspended solids
UASB	Up-flow anaerobic sludge blankets
VOF	Volume of fluid
WWTP	Waste water treatment plant

List of Tables

List of Figures

1 Introduction

An introduction to this project report will be provided in this chapter. The background behind the sewage treatment processes and anaerobic digestion (AD) systems is discussed in the first part of the chapter. A brief overview to the sewage treatment process at VEAS is given in the next section. The main objectives of this thesis and the outline of the report are presented in subsequent sections.

1.1 Background

Environmental pollution has become a growing concern all over the world which has come into the light with the industrial revolution during the past couple of decades. The emergence of large factories and the rapid growth of human population have increased the consumption of fossil fuel and raw materials[1]. This increased consumption cause a large volume of pollutants discharge into the environment daily. Among the different forms of environmental pollution, water pollution has become a major global problem causing large number of deaths and numerous diseases[2]. Water pollution can take place due to the discharge of wastewater from industrial activities into surface water, discharge of domestic sewage and chemical contaminants into surface runoff flowing to surface water and waste disposal and leeching into groundwater[1].

Environmentally safe domestic sewage disposal is a vital factor for preventing water pollution especially in the highly congested cities where huge volumes of sewage being produced daily. Sewage treatment basically involves with the removal of physical, chemical and biological contaminants of sewage in order to produce liquid waste stream and a solid waste which are suitable for safe disposal into the environment or to reuse[3]. A typical sewage treatment plant consists of three stages called primary, secondary and tertiary treatment. The primary treatment generally involves with separating heavy and light solids, oil and grease from the sewage while the secondary treatment removes dissolved and suspended biological matter with the use of water-borne micro-organisms. The purpose of the tertiary treatment is to further improve the quality of the treated effluent before discharging into the receiving environment[3].

Anaerobic Digestion (AD) is a commonly available secondary treatment method to handle the biological wastes in a sewage treatment plant. AD technology not only serves as method to treat biological waste, but also generates biogas as an energy source. It also contributes to reduce the greenhouse gases into the environment[4]. The performance of the AD process is of great interest among the environmental engineers and scientists, in order to improve the biogas yield and the conversion of biological matter. Gas and liquid flow characteristics serve as good indicator to evaluate the performance of the biogas reactors as they directly affect the fluid properties inside the tank. As most of the large scale biogas reactors (also known as

anaerobic digesters) are closed concrete structures, it is very difficult to measure the gas and liquid flow fields inside them. These kind of situations can easily be dealt with Computational Fluid Dynamic (CFD) approach, where models can be used to accurately simulate the flow fields inside large scale reactors[4]. This study has focused on simulating flow fields inside a biogas reactor at VEAS, a large scale wastewater treatment plant which serves a large part of Oslo area and three neighboring municipalities.

1.2 VEAS Wastewater Treatment Plant

Vestfjorden Avløpsselskap, VEAS wastewater treatment plant (WWTP) is an inter-municipal association owned by the municipalities of Asker, Bærum and Oslo, serving more than 450000 residents. VEAS annually treats around 100-110 million m^3 of wastewater.

Wastewater receives into the plant is initial sent through a screening process where most of the large particles such as plastics, cotton swabs and fillers are removed. In the aerated grit chamber, most of the heavier particles like sand are removed. Then some chemicals added to the wastewater stream to remove phosphorous and organic matter. These chemicals allow smaller particles to merge together to form larger flocs which will eventually be settled at the bottom of the sedimentation tanks. The liquid outflow from the sedimentation tank is passed through the nitrogen removal process and finally discharged into the Oslo fjord. The sludge collected at the bottom of the sedimentation tank is sent to the biological treatment process[5, 6].

The sludge from the bottom of the sedimentation tank is passed through rotostrainers, drum thickeners and sludge equalization tank before fed into the anaerobic digesters. The main objective of these three stages is to remove the intertwined fibres, plastics and dissolved solid (DS) matter present in the sludge. The mixed liquor outlet from the equalization tank is then heated to around 36 ^oC and fed into the two stage digester system[5].

The anaerobic digester system at VEAS consists of 4 tanks, each having a volume of 6000 m^3 and filled around 5300 m^3 of liquid. The digestion takes place in two steps, acidification (1-2 days retention) and gas production (17 days retention). Acidification takes place in the first tank while other three tanks are operated in parallel for the gas production step. The generated bio gas is converted into electricity and heat, in a diesel engine. The approximate electricity production is 13 GWh per annum which can contribute to 36% of the power requirement of entire plant. In addition, the recovered heat is sufficient for the heating requirements of the plant and the buildings[5]. A complete flow sheet of the treatment process described above is illustrated in Figure 1-1.

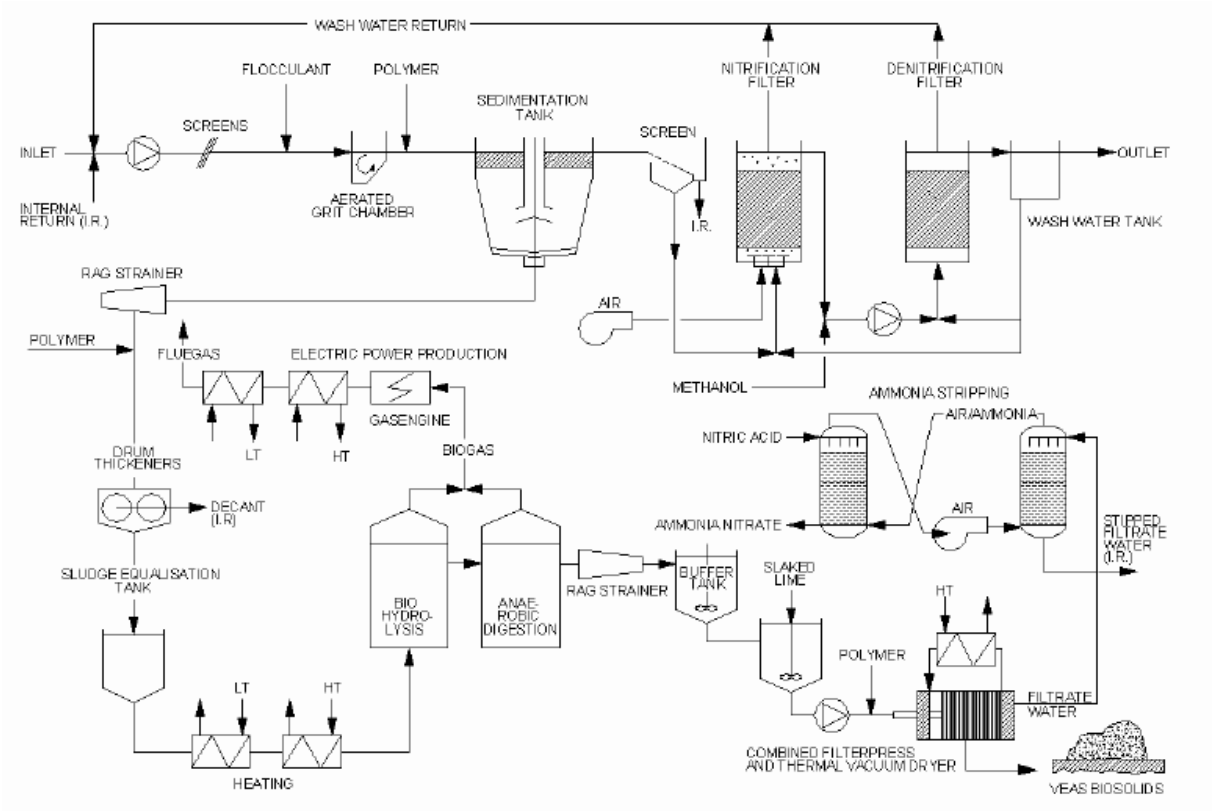

Figure 1-1: Flow sheet of VEAS wastewater treatment process[5].

1.3 Objectives

The main objective of this study is to supplement an ongoing research project carrying out at the Telemark University College in collaboration with VEAS in order to provide recommendations to optimize the wastewater treatment process. As an initial phase of this research project, the following tasks will be covered during this study.

- A Literature review on biogas reactors and gas-liquid flow in tanks to identify the parameters which affects the performances and the flow characteristics of different types of reactors.
- Create a computational mesh of one of the biogas reactors at VEAS using GAMBIT commercial software.
- Simulate the gas and liquid flow in the biogas reactor using ANSYS FLUENT.
- Observe the progression of gas and liquid flow fields over time.
- Investigate the influence of boundary conditions on the flow fields inside the biogas reactor.
- Analysis of the acquired data and a discussion of the behavior of the flow fields.
- Recommend changes in operation and justify these recommendations with the simulation results.
- Provide recommendations for future works.

1.4 Report Outline

At the beginning of the report, a brief introduction is provided to describe the background the main objectives of this study. In chapter 2, a general overview of the biogas reactors and their operation is presented. A literature review of the gas and liquid flow in different reactor configurations similar to this study is presented in Chapter 3. Chapter 4 describes the problem geometry and computational mesh generation process in GAMBIT software. In chapter 5, the complete CFD simulation process and the different cases of study are described. Results of the simulation and discussions are presented in Chapter 6 and Chapter 7 respectively. Conclusions and recommendations for future work are presented in chapter 9.

A list of reference are available at the end of the report followed by a list of appendices from Appendix A to F. GAMBIT files related to the mesh generation, FLUENT case files and screenshots of the process at different time intervals are also attached with this report in electronic format.

2 Biogas Reactors Overview

Biogas is a combustible mixture of gasses which is mainly consists of methane (CH_4) and carbondioxide (CO_2). Biogas is formed from the bacterial decomposition of organic compounds with the absence of oxygen which is also known as anaerobic digestion. The composition of the gasses depends on the biological matter that is being decomposed[7]. Table 1 gives a general idea of the composition of biogas.

Table 2-1: Composition of biogas[7].

Gas	Percentage
Methane (CH_4)	55-70
Carbon dioxide (CO_2)	30-45
Hydrogen sulphide (H_2S) Hydrogen (H_2) Ammonia (NH_3)	1-2
Carbon monoxide (CO)	Trace
Nitrogen (N_2)	Trace
Oxygen (O_2)	Trace

2.1 Advantages of Biogas Technologies

Production and utilization of biogas from the AD offers numerous environmental and socio-economic benefits which are briefly discussed below.

- Renewable energy source

  As the energy demand of the modern world is rapidly growing while the fossil fuel sources have been depleting over time, renewable energy sources has become increasingly important over the recent years. Bio gas generated from the small scale digesters have been widely used as a source of energy for cooking and lighting in developing countries. Most of the European countries use biogas as a source of electricity and heat or directly use as a vehicle fuel[8]. Most of the biogas production facilities utilize the produced heat and electricity to fulfill their own energy requirements.

- Reduced greenhouse gas emissions

  Production of biogas from sewage can reduce the emissions of CH_4 and nitrous oxide (N_2O) which can be produced if the sewage disposed untreated. CH_4 and N_2O have a GHG potential of 23 times and 296 times greater than CO_2 respectively.

- Waste reduction

Transformation of waste material into valuable resources is one of the major advantages of biogas production technologies. As the overproduction of organic wastes has become a huge burden to the society, AD technology is an excellent way to comply with the increasingly restrictive environmental regulations while producing biogas as a valuable energy source and digested substrate as a fertilizer[9].

2.2 Reactor Configurations

Biogas reactors can be designed and operated in different configurations depending on the properties of the fluid being digested, variation of the flow rates and several other factors. The following factors will mainly decide the configuration of a biogas reactor.

2.2.1 Operation

Anaerobic digesters can be designed to operate either as a batch process or continuous process. In a batch process, the reactor is initially fed with the biomass and sealed during its operation. It is a general practice to mix some amount of processed biomass with the batch in order to start the digestion process. The biogas production will generally reach to a peak and start to decrease over time. After the digestion has been completed, the reactor is emptied and fed with a new batch. The batch process considered as a cheaper form of digestion as it is simple to design and requires less equipment[10].

During the continuous process, the biomass is continuously or periodically fed into the reactor while the products (i.e. biogas and digestate) being removed from the reactor, constantly or periodically. Continuous stirred tank reactors (CSTR), expanded granular sludge beds (EGSB) and up-flow anaerobic sludge blankets (UASB) are some common examples of continuous biogas reactors[10].

2.2.2 Operating Temperature

The operating temperature range is a vital factor to decide during the design of the biogas reactors. There are two conventional temperature ranges for the operation of biogas reactors which are mainly depend on the microorganisms present in the biomass.

Mesophilic digestion typically takes place in a temperature range from 25 – 45 ^{o}C with the presence of mesophiles as the primary microorganisms. The optimal temperature range for thermophilic digestion is around 45 – 70 ^{o}C and thermophiles are the primary microorganisms in this process[9]. Mesophilic digestion is considered to be more stable compared to the thermophilic process because of the mesophiles are less prone to the variations of environmental conditions than the thermophiles. In addition, mesophilic systems require comparatively less energy input[10].

Even though the thermophilic systems considered being less stable, it provides faster biogas yields due to the higher reaction rates. High temperature operations also facilitate sterilization of the output digestate[9].

2.2.3 Solid Content

Solid content of the feedstock will also determine the configuration of the reactor. Feed substrate into reactor can be classified into three main types as dry substrate with high solid content, wet substrate with high solid content and wet substrate with low solid content. Dry substrates generally contains between 25 – 40% solid content. This type of substrates are digested in high solid digesters which are built as continuous vertical plug flow or horizontal batch tunnels and operates without the addition of water[10].

In contrast to the dry substrates, wet substrates can be transported with the use of pumps. High solid wet substrates usually having total suspended solid (TSS) content greater than 20% which requires special pumps with high energy input to move and process the fluid.

Substrate with a solid content below 15% is referred as the low solid substrate and it can be easily moved with standard pumps with a significantly lower energy input. But the area required to construct low solid digesters are larger compared to the high solid (wet) digesters because of the higher liquid content[10].

2.2.4 Number of Stages

Anaerobic digestion reactors can be designed as single stage systems or two stage systems. Single stage system is the most popular form due to its less construction cost. But the control over the biogas production process inside the tank is limited since all the key stages of the anaerobic digestion (i.e. Hydrolysis, Acidogenesis, Acetogenesis and Methanogenesis) take place inside a single reactor[10].

In the two stage anaerobic digesters, first three stages of the digestion process supposed to be taken place in the first stage while the biogas will be mainly produced in the second stage from the methanogenesis process. Since the methanogenic microorganisms require a stable pH and temperature, the process can be easily controlled to optimize the performances[10].

"*The biogas reactors at VEAS are operated as a two stage semi-batch arrangement with a feed of wet low solid substrate as described in a previous chapter. As the liquid temperature of the tank is kept at 37 ^{o}C, the digestion process can be assumed as a mesophilic process.*"

2.3 Process Parameters

The efficiency and the performance of anaerobic digestion mainly depend on the parameters such as feed characteristics, feeding patterns, temperature, pH value, nutrient supply, mixing characteristics and the presence of inhibitors[9, 11]. The effect of some of the most important parameters will be briefly discussed below.

- Feed characteristics

  Even though most of the organic matter can be decomposed anaerobically, composition and the properties of the feed will directly affect the performances of biogas production. Organic loading and the microorganisms present in the feed can vary with the different sources and hence affect the yield and the production rate.

- Temperature

  The rate of biogas process generally increases with temperature similar to most of the other biochemical processes. As discussed in section 2.2.2, different microorganisms adapted to different temperature ranges and very sensitive to the changes in temperature which is more significant at elevated temperatures. In addition, the higher temperatures increase the activity of the inhibitors such as ammonia in the system, thus adversely affect the degradation process. On the other hand, viscosity of the liquid is reduced at higher temperatures which facilitates good mixing and diffusion of dissolved materials[7, 9].

- pH value

  pH value in the system mainly influence the growth of the methanogenic bacteria. The optimum pH range for the methanogens to operate is between 6.5 and 8 and but the preferred value is a pH of 7.2[7].

- Mixing characteristics

  Stirring or mixing is an important parameter in most of the digesters in order to prevent the formation any impenetrable surface crusts, to facilitate better contact between microorganisms and the biomass and to maintain the homogeneity of the liquid with respect to temperature and pH. The importance of mixing will be further discussed in a latter section of this report.

- Inhibitors

  Inhibitors are the substances which influence a system in a negative manner. Higher ammonia content inside the digester can affect the methanogens activity on biomass. Toxic compounds, antibiotic and disinfectant agents present in the feed are also considered as inhibitors for the biogas production process[7, 9].

2.4 Importance of Mixing

Efficient mixing has been proved to increase the performance and efficiency of the biogas systems during numerous commercial applications and research studies[4]. Mixing in an anaerobic digester is a vital factor to achieve a uniform temperature and pH in the liquid, dilute inhibitory substances, transfer substrate to microorganisms and to prevent stratification and short circuiting [11]. Mixing inside the biogas reactors can be achieved by either mechanical mixing, slurry recirculated mixing or biogas mixing. Combinations of these methods are also employed in certain circumstances.

Biogas mixing is preferred over mechanical mixing and slurry recirculated mixing in several applications as it is less expensive and easier to operate compared to other two types[4]. Due to the absence of moving parts, the problems such as wear and tear are avoided. Biogas mixing also accommodates excellent heat and mass transfer characteristics inside the liquid[12].

Importance of mixing has been extensively studied during several research works in the literature[4, 11]. According to the studies of Latha *et al*., the main factors affecting the digester mixing are mixing intensity and duration, the location of the feed inlet and outlets and the type of mixing[4]. The research works of Latha *et al*. and Terashima *et al*. reveals contradictory results from different literature regarding the adequate amount of mixing[4, 11]. Adequate mixing enhances the distribution of substrates, enzymes and microorganisms while inadequate mixing results in stratification and formation of floating layers of solids inside the digesters. Continuous mixing was observed to improve biogas production compared with the unmixed reactors[4]. On the other hand, high mixing intensities shown to disrupt the structure of microbial flocks due to the excessive shear, thus cause performance deterioration in the reactor[4].

Therefore, achieving an appropriate level of mixing will be a crucial factor during the operation of anaerobic digesters.

3 Gas Liquid Flow in Reactors

The main objective of this study is to identify the flow characteristics inside the biogas reactors at VEAS. Experimental approaches to this kind of situations are not very promising as the reactors are very large in dimension, sealed during the operation and made out of concrete which make is impossible to observe from the outside.

Computational Fluid Dynamics (CFD) plays a major role in design and optimization of various reactors, as it allows investigating the local conditions inside the arbitrary vessels of different size, geometry and operating conditions. CFD techniques can predict the detailed flow fields inside the reactors in order to evaluate mixing time, power consumption, flow patterns and velocity profiles associated with them[13].

The flow inside the biogas reactors at VEAS can be treated as a gas liquid flow because of the biogas mixing and the feed being a liquid with very little amount total suspended solids. Gas liquid flow also referred to as two phase flow which is a subset of multiphase flows. Gas liquid flows can be identified in numerous industrial applications within agricultural, biochemical, chemical and pharmaceutical industries[13].

A proper literature review on the application of CFD techniques to simulate the gas liquid flow inside different industrial and experimental reactors is necessary to adapt appropriate numerical methods for this study. Even though the studies related to the bio gas distribution arrangements similar to this study are quite rare in the literature, other types of gas liquid flow arrangements in various reactor geometries are readily available. Gas lift reactors and bubble column reactors, generally identified as diffused air systems, display somewhat similar gas flow arrangement to the VEAS biogas reactors. Therefore, a brief overview of these reactor types together with the applications of CFD techniques to simulate the flow fields inside them is presented in the following sub sections.

3.1 Bubble Column Reactors

Bubble column reactors are widely used in several industrial applications due to their simple construction, less operating and maintenance cost associated with the absence of internals or moving parts, effective mixing and the better heat and mass transfer capabilities. The gas phase serves as a medium for aeration and agitation. The reactor is initially filled with liquid and the gas phase is aerated through the bottom of the tank by perforated plates or diffusers[13]. A simple schematic of a bubble column is illustrated in Figure 3-1.

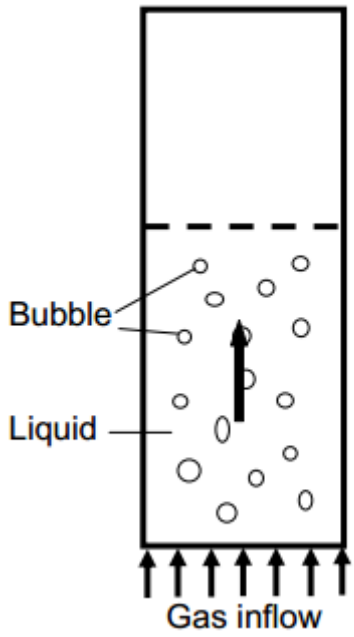

Figure 3-1: Schematic of a simple bubble column[13].

The literature studies reveal that the performance of bubble column reactors mainly depends on the gas holdup, bubble size, bubble rise velocity, bubble-bubble interactions and mixing rate. Extensive amount of literature works are available to assess the effect of these parameters on the performance of the bubble column reactors and to identify the flow characteristics inside them. Zhang carried out a comprehensive study of the interfacial closure laws and multiphase turbulent models in modeling of gas liquid flow in bubble columns[14]. Buwa *et al*. have performed various research works on bubble columns and studied the role of unsteady flow structures in liquid phase mixing and dynamic characteristics of oscillating bubble plumes using experiments and CFD simulations. Three dimensional rectangular bubble columns were used in their simulations and both Euler-Euler and Euler-Lagrange approaches were employed[15, 16]. The studies of Akhtar *et al*. mainly focused on the effect of various sieve plate gas distributors and gas superficial velocities on the hydrodynamics of three dimensional flows in bubble columns[12].

3.2 Gas/Air Lift Reactors

One disadvantage of the bubble columns in the applications such as biological fermentation and waste water treatment is the incapability of achieving homogeneous liquid at low superficial velocity especially in three phase flow regimes. This kind of situation can be avoided with the liquid recirculation inside the column with the use of air lift reactors. Air lift reactors offer same advantages as the bubble columns but also provide some additional benefits too. The control over the liquid circulation to reduce back mixing, reduced liquid shear stress which facilitates shear sensitive microorganisms are some of them[13]. Air lift

reactors can be designed as internal air lift reactors (ILALR) and external air lift reactors (ELALR) as illustrated in Figure 3-2[13].

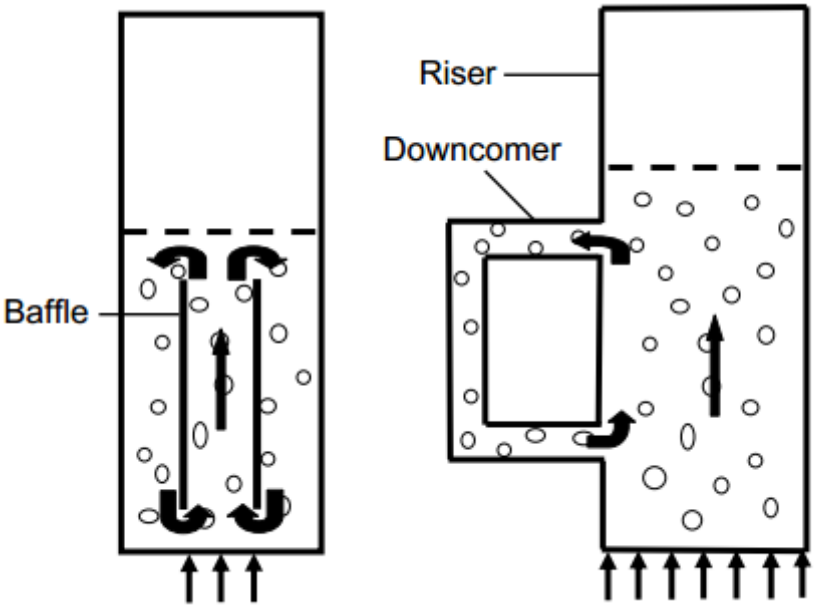

Figure 3-2: Schematic of internal and external air lift reactor[13].

ILALR consists of a draft tube or baffles in the bubble column while the ELALR composed of two vertical columns connected together with horizontal connectors to form a loop. The column can be divided into two parts as riser and downcomer. Gas phase is generally introduced and rise up through the riser section and then travels to the bottom of the column through downcomer section to enter the riser section again. This will allow the liquid phase to circulate continuously around the loop thus providing better mixing[13].

Research studies of the CFD simulations of air lift reactors are also available in the literature. For example, Hekmat et al. simulated the flow inside a draft tube air lift reactor (or ILALR) to determine the optimum distance to the draft tube from the wall using Euler-Euler approach[17]. A broad study has been carried out by Law on computational modeling and simulation of hydrodynamics for external airlift reactor during his research works[13].

3.3 Factors Affecting Diffused Air System Performances

Optimization of the performance of anaerobic digesters is essential to increase the biogas yield and the decomposition of the biological waste. Studies related to the performance of general diffused air systems are also applicable to this particular project as the biogas reactor configuration at VEAS can be considered as a diffused air system.

In diffused air systems, gas phase is introduced to the mixed liquor through the diffusers which are normally located at the bottom of the tank. Depending on the bubble size distribution, diffused air systems are classified as coarse or fine bubble systems. 2-5 mm

bubble size distributions can be considered as fine bubbles while 6-10 mm bubble size distributions can be treated as coarse bubbles[18]. Some important factors affecting bubble diffused air systems are,

- Tank geometry and diffuser placement

  A vertical circulation of liquid is generated by the air lift pumping effect of the air bubbles released from the diffuser outlets. The circulation of liquid depends of the tank geometry and the position of the diffusers. Diffusers positioned at one side of a tank provide better mixing input to the entire tank than uniformly distributed ones[18].

- Diffuser density and gas flow rate

  Diffuser density and gas flow rate directly control the generation of gas bubbles inside the system. Increasing both parameters to higher values will provide rigorous mixing which may be unfavorable for the microorganism growth.

- Contaminants in the liquid

  Presence of contaminants such as surfactant can reduce the surface tension of liquid and thus reducing bubble size and hindering bubble coalescence[18].

- Diffuser fouling

  Fouling can be mainly caused by clogging of diffuser openings with particulate material inside the mixed liquor. Reduced gas flow rates, increased head loss and increased energy consumption are main disadvantages of fouling[18].

4 Reactor Geometry

The initial and the most important step of any CFD analysis is the construction of problem geometry and generation of computational mesh. The accuracy of the solution and the rate of convergence directly associated with the quality of the computational mesh. This chapter will mainly discuss the dimensions of the reactors at VEAS and the generation of the 3D reactor geometry and the computational mesh in GAMBIT 2.4.6 commercial software, a preprocessor for FLUENT.

4.1 Reactor Dimensions

Mechanical drawings of one of the biogas reactors at VEAS are illustrated in Figure 4-1and Figure 4-2.

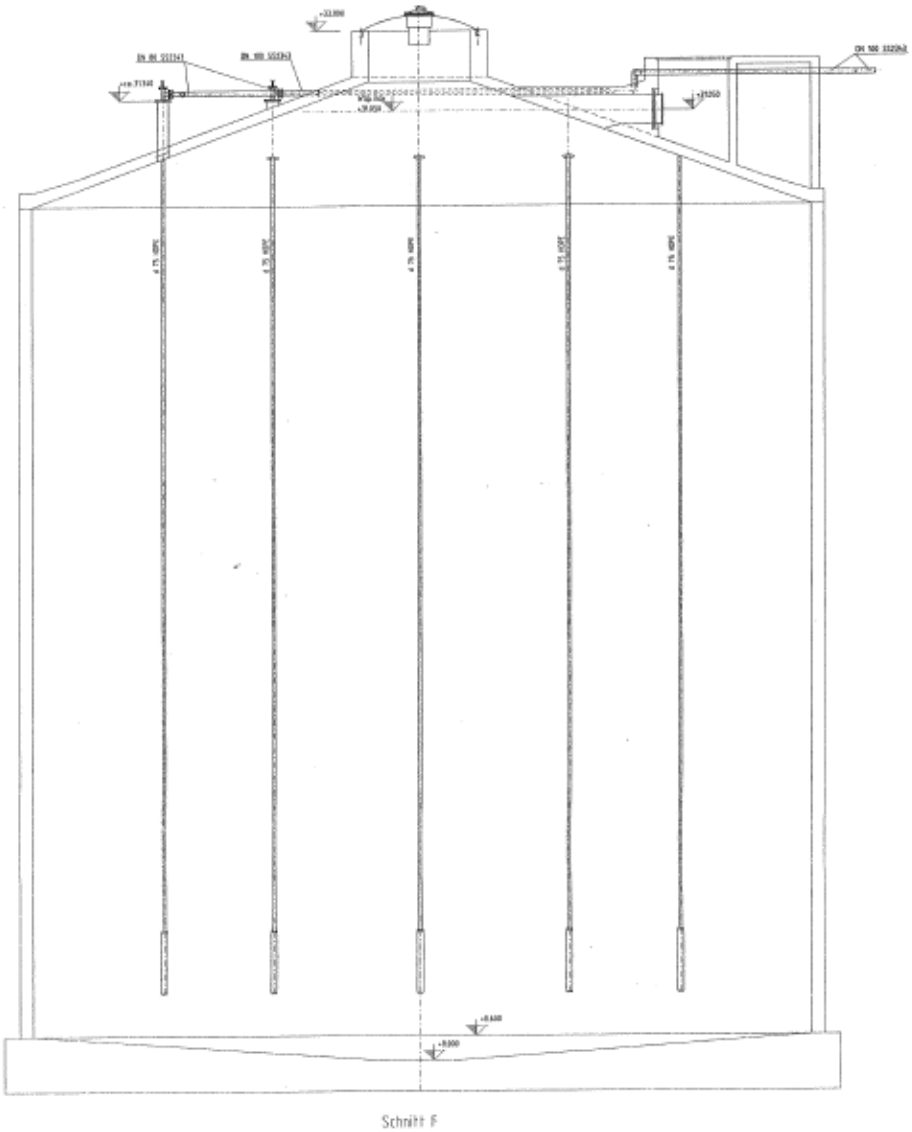

Figure 4-1: Side view of a biogas reactor at VEAS[19].

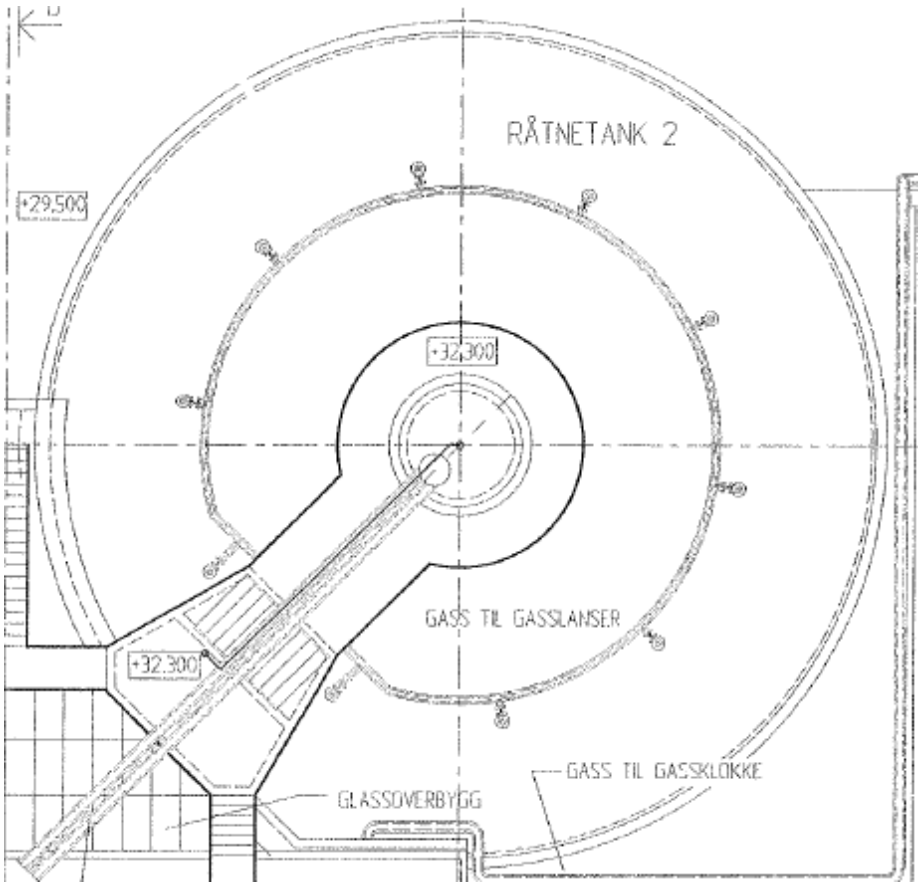

Figure 4-2: Plan view of a biogas reactor at VEAS[19].

All the necessary dimensions which were used to create the 3D geometry of the reactor are listed in Table 4-1.

Table 4-1: Biogas reactor dimensions.

Parameter	Value
Reactor internal diameter	19 m
Total liquid height	20.75 m
Height of the cylindrical section	20.15 m
Height of conical frustum section	0.6 m
Radius 1 of conical frustum section	9.5 m
Radius 2 of conical frustum section	1 m
Number of pipes	10 (Equally spaced at 36^{o})
Distance to the pipes from central axis	6.3 m
Distance to the inlets from the bottom of the cylindrical section	1 m

Cross sectional, three dimensional and cross sectional views of the created geometry are shown in Figure 4-3.

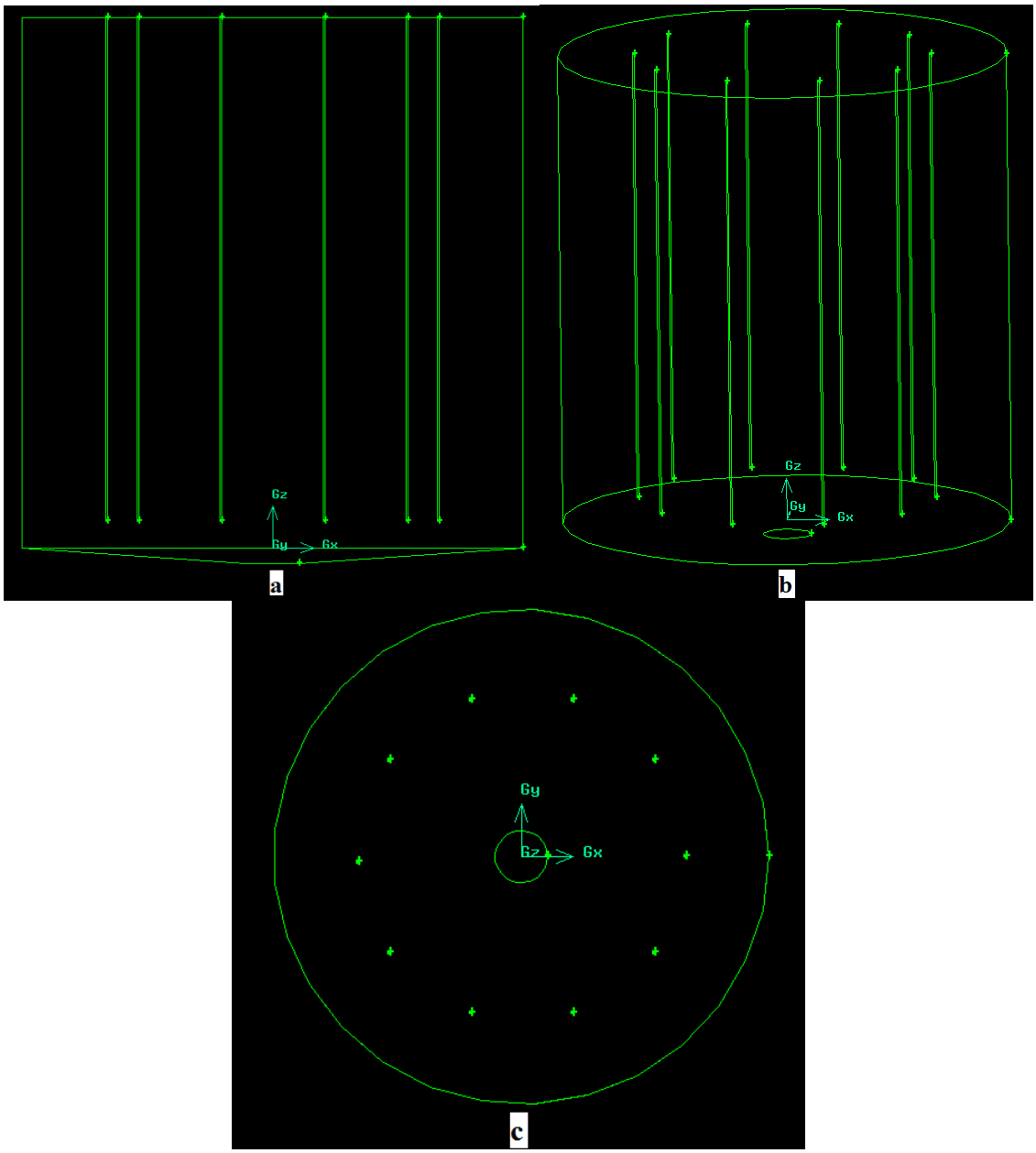

Figure 4-3: Reactor geometry in GAMBIT a) Side view b) 3D view c) Plan view.

4.2 Computational Mesh

Meshing of the geometry was done as two separate volumes to overcome certain incompatibilities. The reactor volume was divided into two parts across Z=1 m plane. The major constraint during the meshing of the top volume was the smaller dimensions of the pipes compared to the tank diameter. Therefore, meshing of the top volume was done with a great care to achieve a fine mesh around the pipes and coarser mesh in the rest of the volume. The basic steps of the mesh generation of the top volume are as follows.

- Boundary layer mesh inside the gas inlet surface of the pipes and a surface mesh for the rest of the surface area.
- Surface mesh along the pipes to the top using Tri Pave option with 0.3 m interval size.
- Mesh the top volume with tetrahedral elements (unstructured) TGrid type and 0.5 m interval size. This resulted in a finer mesh around the pipes and coarser mesh in rest of the volume.
- Mesh the bottom volume with tetrahedral elements similar to the top volume. A finer mesh was generated around the gas inlets (pipe bottom surfaces) while a coarser mesh was generated for the rest of the volume.

The final mesh consists of 1,273,914 elements with a reasonable quality. The skewness of the worst element was 0.897 and only 1% of the total elements exceeded the skewness of 0.715. Figure 4-4 illustrates a side view and a 3D view of the computational mesh. Figure 4-5 shows the mesh layout at Z=1 plane where gas inlets are located. A very fine mesh around the pipes and a coarse mesh in rest of the area can be observed from the figure.

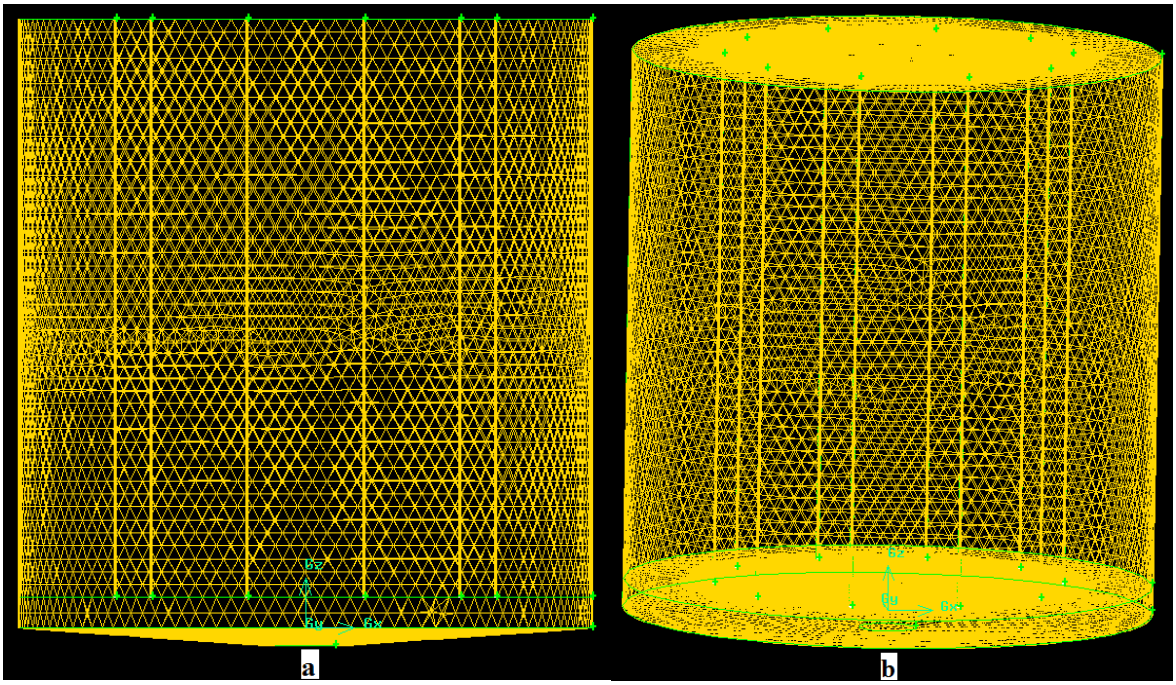

Figure 4-4: Computational mesh of the biogas reactor a) Side view b) 3D view

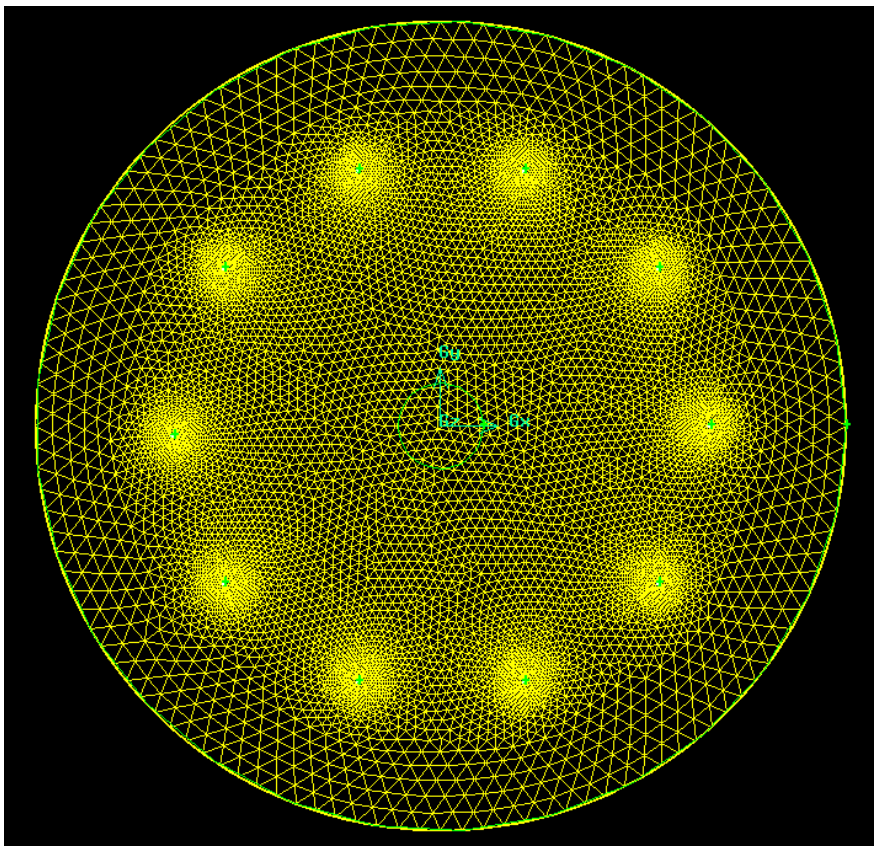

Figure 4-5: Computational mesh on Z=1 plane.

5 CFD Simulations

A commercial CFD software FLUENT 13.0 (ANSYS, Inc., USA) release version was used to simulate the flow fields in the biogas reactor under different boundary conditions. Selection of the appropriate simulation parameters is essential to get a good representation of the actual flow characteristics inside the biogas reactors. This chapter will mainly discuss the criteria for selection of flow regime and multiphase model, simulation procedures and the different cases of simulation.

5.1 Selection of Flow Regime

According to the ANSYS Fluent user documentation[20], multiphase flow regimes can be grouped in to four main categories.

- Gas-Liquid or Liquid-Gas flow
  - ✓ Bubbly flow - discrete gaseous or fluid bubbles in a continuous fluid.
  - ✓ Droplet flow - flow of discrete fluid droplets in a continuous gas.
  - ✓ Slug flow - flow of large bubbles in a continuous fluid.
  - ✓ Stratified/Free surface flow - flow of immiscible fluids separated by a clearly-defined interface.
- Gas- solid flow
  - ✓ Particle-laden flow - flow of discrete particles in a continuous gas.
  - ✓ Pneumatic transport - This is a flow pattern that depends on factors such as solid loading, Reynolds numbers, and particle properties.
  - ✓ Fluidized bed - Consists of a vertical cylinder containing particles, into which a gas is introduced through a distributor. The gas rising through the bed suspends the particles.
- Liquid – solid flows
  - ✓ Slurry flow - This flow is the transport of particles in liquids.
  - ✓ Hydrotransport - This describes densely-distributed solid particles in a continuous liquid
  - ✓ Sedimentation - This describes a tall column initially containing a uniform dispersed mixture of particles. At the bottom, the particles will slow down and form a sludge layer. At the top, a clear interface will appear, and in the middle a constant settling zone will exist.
- Three – Phase flow - combinations of the other flow regimes listed above.

As far as biogas reactors are considered, large number of research works had been carried out with different multiphase flow regimes. The selection of the multiphase flow regime is mainly depends on the number of phases involves with the process and properties of the fluids being considered. For the systems involving wastewater with high biomass content, three-phase flow is preferred in literature where wastewater is considered as the primary phase and the gas and the sludge granules are considered as secondary phases[21]. There are some other literature which has modeled the reactor content with a continuous liquid phase and secondary gas phase[4].

In the VEAS wastewater treatment plant, most of the solid content of the sewage is removed before it is fed into the biogas reactors. Hence the content inside the reactor can be easily considered as a continuous liquid phase. Also, as the mixing inside the tank is achieved by pumping a portion of the produced biogas back into the tank using 10 pipes, biogas is considered as a secondary gas phase. Therefore, the flow inside the biogas reactor in this particular study is assumed as a liquid-gas bubbly flow.

Due to the lower solid concentration, the liquid inside the tank can be considered as water and the physical properties of water have been used during the simulation process. In addition, properties of air have been used instead of biogas for the simplicity of the simulation process.

5.2 Selection of General Multiphase Model

Numerical calculations take an important role in predicting dynamics of multiphase flows in computational fluid mechanics. There are two approaches for numerical calculations of multiphase flows as Euler-Euler approach and Euler-Lagrange approach.

5.2.1 Euler-Euler Approach

In the Euler-Euler approach, different phases are treated as interpenetrating continuous mediums and a concept of volume fraction of phases is introduced. The volume fractions of each phase are assumed to be continuous functions of time and space and their sum is equal to one. Conservation equations are derived to obtain a set of similar equations for all the phases[20]. In Fluent application, three types of Euler-Euler multiphase models are available for different kind of applications.

- VOF Model

  VOF model is designed for two or more immiscible fluids and deals with the positions of the interface between these fluids. In this model, a single set of momentum equations are used for all the fluids and the volume fraction of each of the fluids is tracked throughout the calculation domain[20].

  Typical Applications: Stratified flows, free-surface flows, filling, motion of large bubbles in a liquid

- Mixture model

  Mixture model is generally used for two or more phases and these phases are treated as interpenetrating continuous mediums. This model calculates mixture momentum equation to provide relative velocities for the dispersed phases[20].

  Typical Applications: Particle laden flows with low loading, sedimentation, cyclone separators, bubbly flows

- Eularian Model

  "The Eulerian model is the most complex of the multiphase models in ANSYS FLUENT. It solves a set of momentum and continuity equations for each phase. Coupling is achieved through the pressure and interphase exchange coefficients. The manner in which this coupling is handled depends upon the type of phases involved. Momentum exchange between the phases is also dependent upon the type of mixture being modeled"[20].

  Typical Applications: Bubble columns, risers, particle suspension, fluidized beds

5.2.2 Euler – Lagrange Approach

In Euler-Lagrange approach, the fluid phase is considered as a continuous medium while the dispersed phase is treated as separate particles in contrast to the Euler-Euler approach. This approach involves with tracking large number of separate particles, bubbles or droplets which can exchange mass, momentum and energy with the continuous phase. This makes Euler-Lagrange approach more CPU intensive than the Euler-Euler approach[20]. At an increased computational effort, the following advantages can be achieved from the Euler-Lagrangian approach[15].

- More accurate description of inter-phase forces by evaluating bubble size distributions in a simple manner
- Bubble-bubble interactions and bubble induced turbulence can be modeled in a realistic way.
- Possibility to model transport processes and reactions which take place around and within individual bubbles.

Generally, an Euler-Lagrange method is not recommended for designing large reactors and for the systems having high volume fraction of the dispersant phase[17]. Some common applications of this approach are modeling of spray driers, coal and liquid combustion and some particle laden flows[20].

5.2.3 Selection of Appropriate Multiphase Model

Three criteria have been taken into consideration during the selection of most appropriate multiphase model for this particular study.

- Recommendations from the ANSYS FLUENT application.

- Literature works carried out on similar cases.
- Complexity of the geometry and the estimated CPU time and required computer resources.

ANSYS FLUENT application recommends Eularian and mixture models for bubble flow applications. On the other hand Euler-Lagrange approach is also preferred for the similar cases as this study where the dispersed phase volume fractions less than 10%. Several research works have been carried out for systems having bubble flow characteristics in both Euler-Euler approach[12, 17] and Euler-Lagrange approach[4, 15].

"*But taking into account of the facts that the bulkiness of the reactor geometry having over 1.2 million control volumes and evaluation of the interaction between individual bubbles is not an interest of this study, Euler-Euler approach has been selected to reduce the computational effort and speed up the simulation process."*

5.3 Simulation Steps

Computers with Intel® Core™ i5-2500 CPU @ 3.30 GHz 3.30 GHz processors, 8.00 GB memory and Windows 7 Enterprise Edition 64 bit operating system were used to run the simulations. Average simulation times for different cases were in the range of 3-5 days to achieve about 1 hour of flow time. The simulation procedure includes the following steps.

- Import the mesh file generated from GAMBIT into FLUENT and check the mesh for any incompatibilities.
- Define the solver as pressure-based and transient.
- Define the multiphase model as Eularian with two phases.
- Select standard k-epsilon model as the viscous model and keep the default values for the model constants.
- Define the materials, liquid and biogas with the same properties as water and air respectively. For the biogas, select "ideal-gas" as the density method.
- Select liquid as the primary phase and biogas as the secondary phase. Bubble diameter of the secondary phase is set as 0.001 m, 0.005 m or 0.01 m depending on the case.
- Define the appropriate boundary conditions at the velocity inlet and the pressure outlet depending on the case. A detailed description will be presented in a latter section.
- Set the operating pressure to 0 Pa, activate gravitational acceleration on Z axis and set the specified operating density to 0 kg/m^3 in operating conditions window.

5.4 Simulation Cases

Simulations were carried out for different cases to investigate the influence of boundary conditions and other parameters on the stability of the solution and the flow fields inside the reactor. Most of the cases were run with a simple gas distribution arrangement which employed all 10 pipes to supply a continuous gas flow into the liquid volume.

5.4.1 Bubble Diameter

As there were very little information about the liquid gas flow inside similar scale biogas reactors, having an idea of the average bubble diameter and the bubble size distribution is crucial during this study. The size of an average bubble and bubble size distribution depend on the factors such as distributor diameter, properties of the liquid and gas flow rate. As the diameter of the distributor (pipe) is large compared to most of the cases available in the literature, it was decided to run the simulations with three different bubble sizes of 1mm, 5mm and 10mm in order to check the stability of the solution as well as the flow patterns. For each of these cases, velocity contours of both liquid and gas have been obtained at different time intervals to observe the flow fields inside the tank and to check the time which the system takes to achieve a stable velocity profile.

- 1 mm bubble diameter

  Initially 1 mm bubble size was used as the secondary phase diameter. The simulations were carried out in transient state with 0.001 s as the initial time step size. The time step size was gradually increased through 0.005 s, 0.01 s, 0.05 s, 0.1 s, 0.5 s and 1 s as the system get stabilized over the time.

- 5 mm bubble diameter

  5 mm bubble size case was also started with 0.001 s time step size and gradually increased up to 1 s as the systems get stabilized.

- 10 mm bubble diameter

  Finally, 10 mm bubble size was used to simulate the gas liquid flow inside the biogas reactor. Same approach as the previous two cases has been used to achieve a faster convergence of the solution.

5.4.2 Inlet Gas Velocity

Inlet gas velocity mainly depends on the gas flow rate, diameter of the pipes and the number of pipes used during the gas distribution. During the initial simulations which used simple 10 pipe gas distribution arrangement, the gas velocity was calculated as 1.2 m/s (see Appendix B for calculations) for the given gas flow rate of 300 Nm^3/h. During the actual operation of the

reactor at VEAS, only 5 pipes at a time is used to distribute gas inside the reactor, hence the inlet gas velocity will be doubled (i.e. 2.4 m/s).

Apart from the initial gas velocity of 1.2 m/s, a lower gas velocity of 0.6 m/s which corresponds to half of the gas flow rate (150 Nm^3/h) was also used to compare the results. Due to the time constraints of this study and limited computer resources, only the 5 mm bubble size was simulated with 0.6 m/s gas velocity.

5.4.3 Source Term

Operational data from biogas reactors shows that each biogas reactor produces around 320 Nm^3/h of biogas during its normal operation. This process will also contribute to the generation of gas bubbles inside the liquid volume. Therefore, bio gas generation was also included in the simulation as a source term of $2*10^{-05}$ $kg/m^3.s$ (See Appendix C for calculations) to observe its effect on flow patterns inside the tank. The comparison was done with 5mm bubble diameter and initial gas distribution arrangement.

5.4.4 Actual Gas Flow Arrangement

Actual operation of the biogas reactors at VEAS is bit different than the initial simulations of this study which were carried out to understand the general flow patterns and optimum simulation conditions.

Bubbling of gas inside the tank is performed in an alternating manner instead of using all the 10 pipes at a time. Initially only 5 neighboring pipes are used to pump air into the reactor for 15 minutes. Then the bubbling process stops for around 5-10 minutes. Again the gas sends through the next 5 pipes for another 15 minutes. This cycle continues throughout the operation of the biogas reactor. Figure 5-1 illustrates the general operational pattern of the reactor.

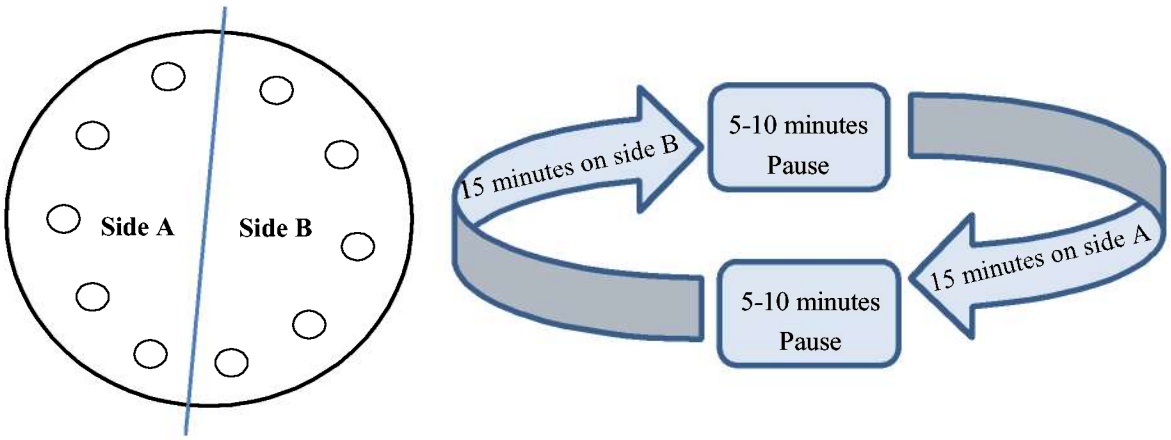

Figure 5-1: Actual gas distribution sequence at VEAS biogas reactor.

The original mesh was updated to have two velocity inlet boundaries (each consist of five neighboring inlet pipes). During the simulations, only one velocity inlet was used with inlet

gas velocity of 2.4 m/s (twice the inlet velocity of previous cases) for around 15 minutes of flow time. Then the gas bubbling process paused for another 7 minutes (i.e. velocity of the both inlets set to 0 m/s) and finally the second velocity inlet has been employed for another 15 minutes. Only the 10 mm bubble size was simulated with this arrangement as the simulations took very long time to complete.

5.5 Boundary Conditions

Since one of the main objectives of this study is to investigate the influence of boundary conditions on the flow field inside the reactor, different boundary conditions were used depending on the cases described in the previous section. Some of the boundary parameters were kept constant for all the cases. The following sections will briefly describe the boundary conditions used during the simulations.

5.5.1 Velocity Inlet

Two velocity inlet types were used for the simulations. For the initial cases, all the 10 gas inlets were considered as one velocity inlet and it was assumed that biogas is fed from all the inlets. For the actual gas flow arrangement, two velocity inlets were used as discussed in the section 5.4.4. Following parameters were kept constant for all the cases.

- Mixture phase

  Initial gauge pressure was set to 0 Pa. Turbulent intensity was assumed as 10% and the hydraulic diameter was set to 0.075 m which is the diameter of the pipe.

- Liquid phase

  Liquid velocity of the inlet was set to 0 m/s.

- Biogas phase

  Velocity magnitude of the gas normal to the boundary was set as 0, 0.6, 1.2 and 2.4 m/s depending on the case. Temperature of the inlet gas was set to 340 K and the volume fraction of the gas at the inlet was defined as 1.

5.5.2 Pressure Outlet

The same pressure outlet conditions were used for all the simulations which are briefly discussed below.

- Mixture phase

  Gauge pressure was defined as 105325 Pa. Turbulence at the pressure outlet was characterized with backflow turbulent intensity of 5% and backflow turbulent viscosity ratio of 5.

- Liquid phase

  Backflow total temperature was set to 310 K.

- Biogas phase

  Backflow volume fraction of the gas was set to 0 which will prevent liquid entrainment with gas at the boundary.

5.5.3 Wall

The default no slip conditions were kept unchanged at the wall for both liquid and biogas phases.

6 Simulation Results

Simulations for each case were carried out for at least 1 hour of flow time in order to observe the variation of flow fields over time. Velocity contours at Y=0 m plane (the vertical plane passing through the center of the tank) of both liquid and gas were plotted in predefined time intervals throughout the simulations process. Liquid velocity vectors were also obtained at the same plane to investigate the liquid flow directions inside the reactor after the simulations reach a stable state. In addition, the velocity contours at Z=1, 6, 12 and 18 m (horizontal cross sections of the tank at different liquid heights) were observed at the end of the simulations. Furthermore, liquid velocity distributions across the diameter of the reactor along A-A line (See Figure 6-1) at different liquid heights (i.e. Z=1, 6, 12, 18 m) were observed using XY plots. Gas volume fraction profiles were obtained for some of the cases Moreover, gas velocity contours and gas velocity distribution plots for all the cases were presented in Appendix E & F respectively.

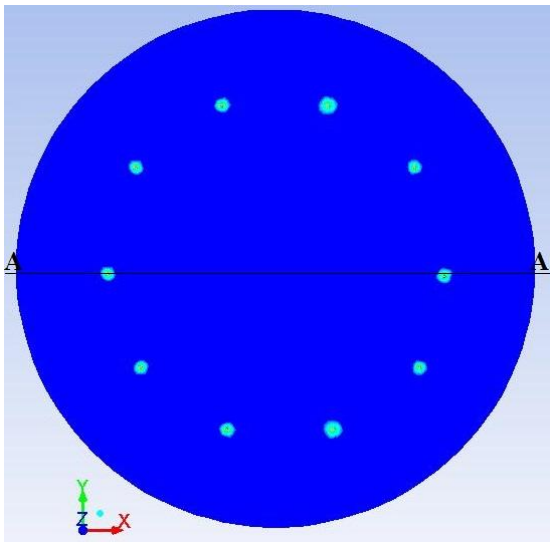

Figure 6-1: A-A line across which the XY plots of velocity magnitudes were obtained for initial gas distribution arrangement.

6.1 Effect of Gas Bubble Size

Progression of the flow fields over time, liquid and gas velocity contours of both liquid and gas at four horizontal planes, velocity distribution across the diameter of the tank and liquid velocity contours and liquid velocity vector profiles at the end of the simulations are presented for all the three cases of 1 mm, 5 mm and 10 mm in the following sections.

6.1.1 1 mm Bubble Size

Figure 6-2 illustrates the liquid velocity development inside the reactor for 1 mm bubble size at different time stages.

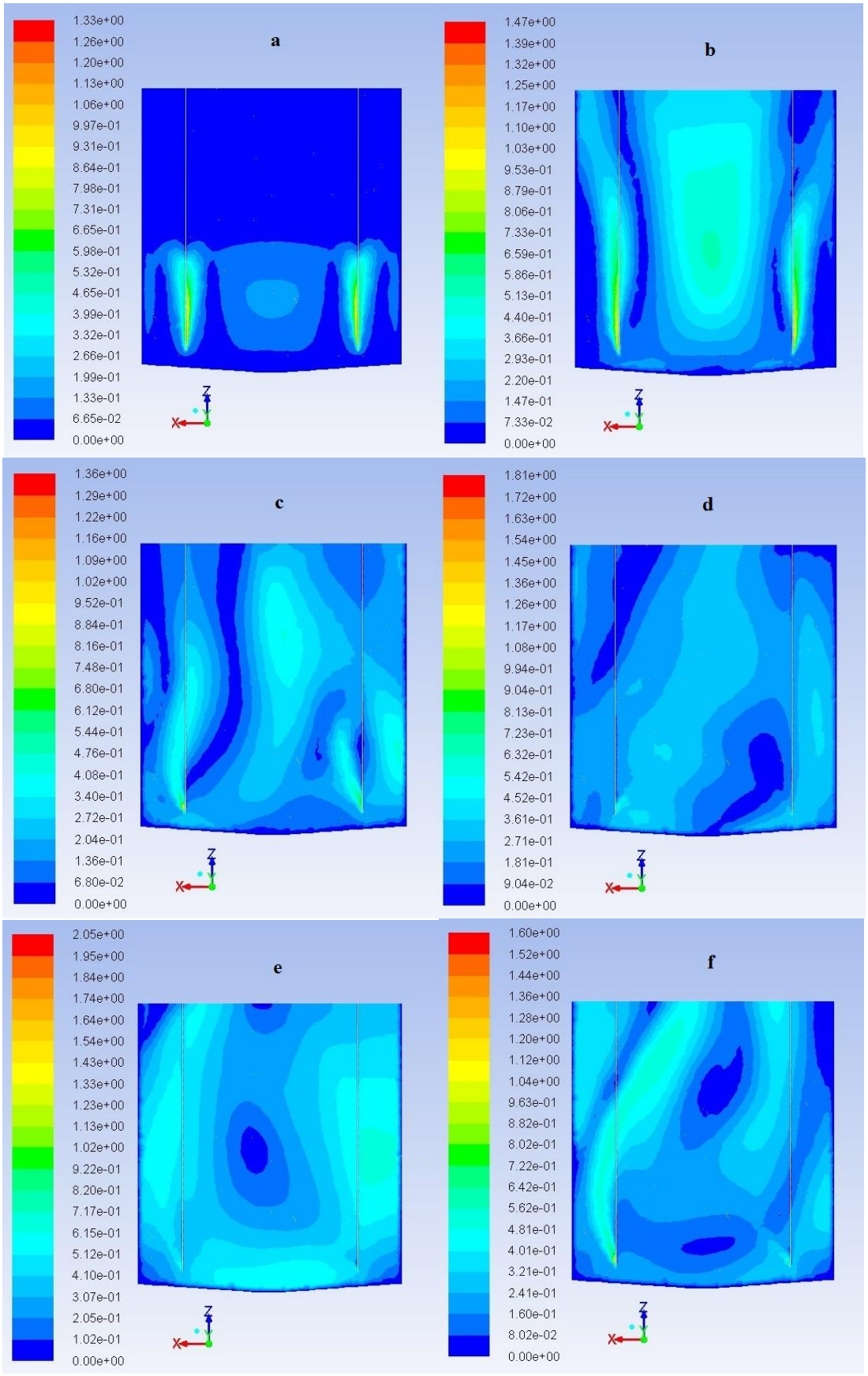

Figure 6-2: Evolution of liquid velocity profile for 1mm bubble size at a) 60 s b) 180 s c) 300 s d) 600s e) 1000 s f) 1800s.

Liquid and gas velocity contours of horizontal planes Z=1, 6, 12 and 18 m are illustrated in Figure 6-3. Figure 6-4 shows the liquid velocity distribution across the tank diameter at different liquid levels.

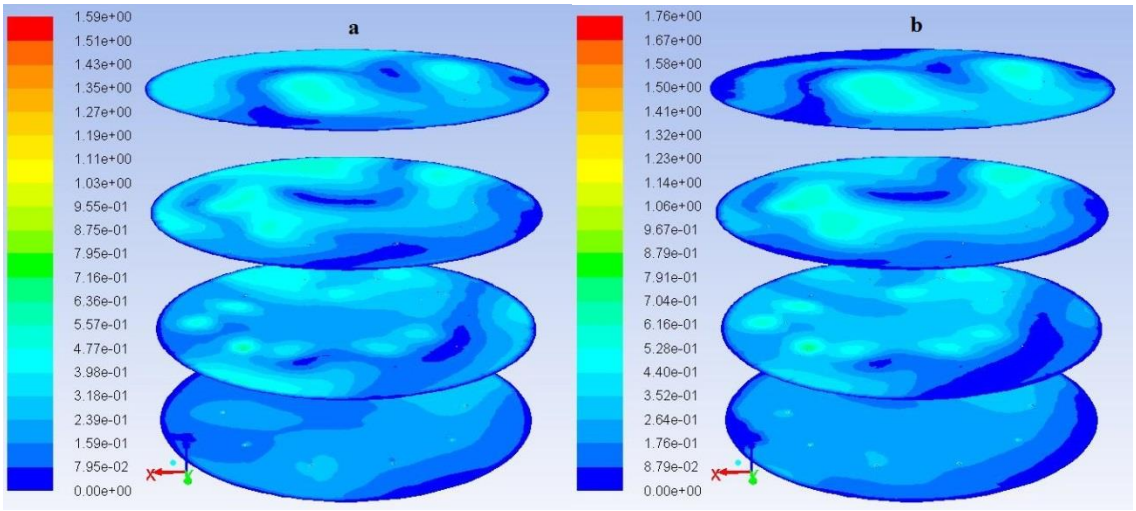

Figure 6-3: a) Liquid velocity b) Gas velocity contours at Z=1, 6, 12, 18 m planes for 1 mm bubble size after 1800 s of flow time.

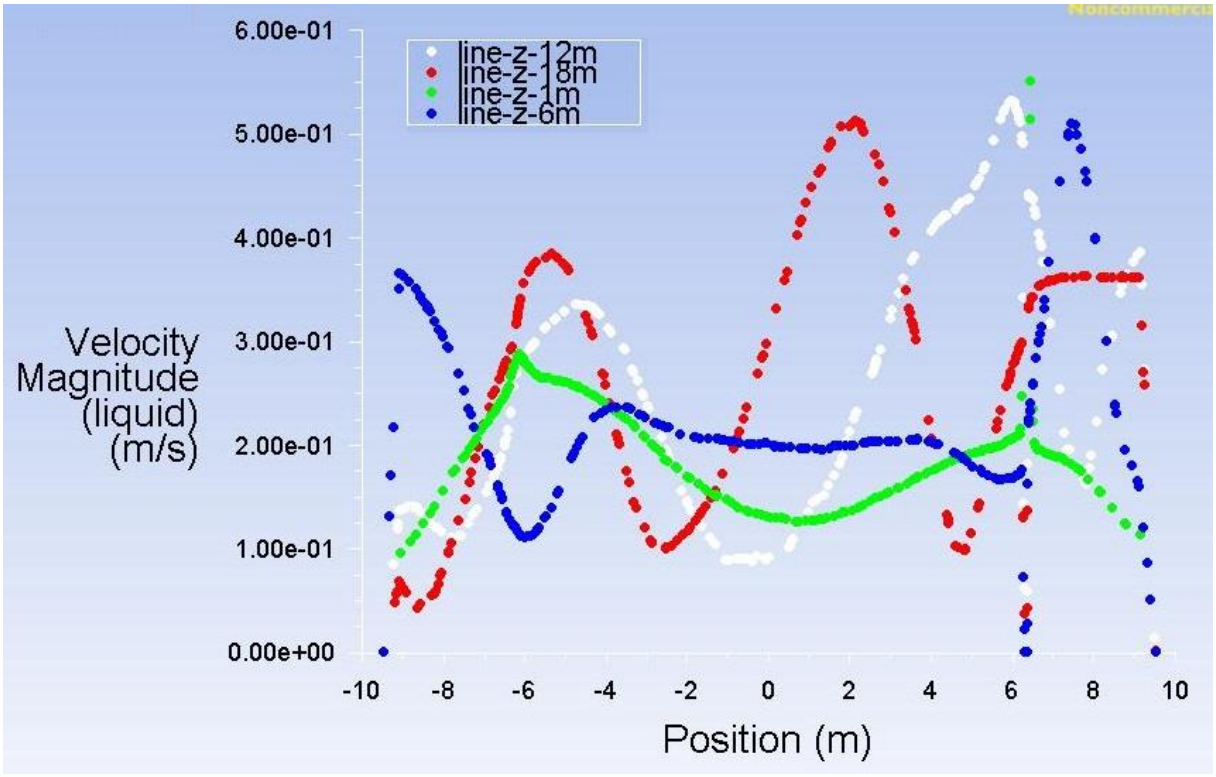

Figure 6-4: Liquid velocity distribution across the diameter of the tank at Z= 1, 6, 12, 18 m for 1 mm bubble size after 1800 s of flow time.

Liquid velocity contour and liquid velocity vector profile was obtained at the end of the simulation to observe the liquid flow distribution and direction which is presented in Figure 6-5.

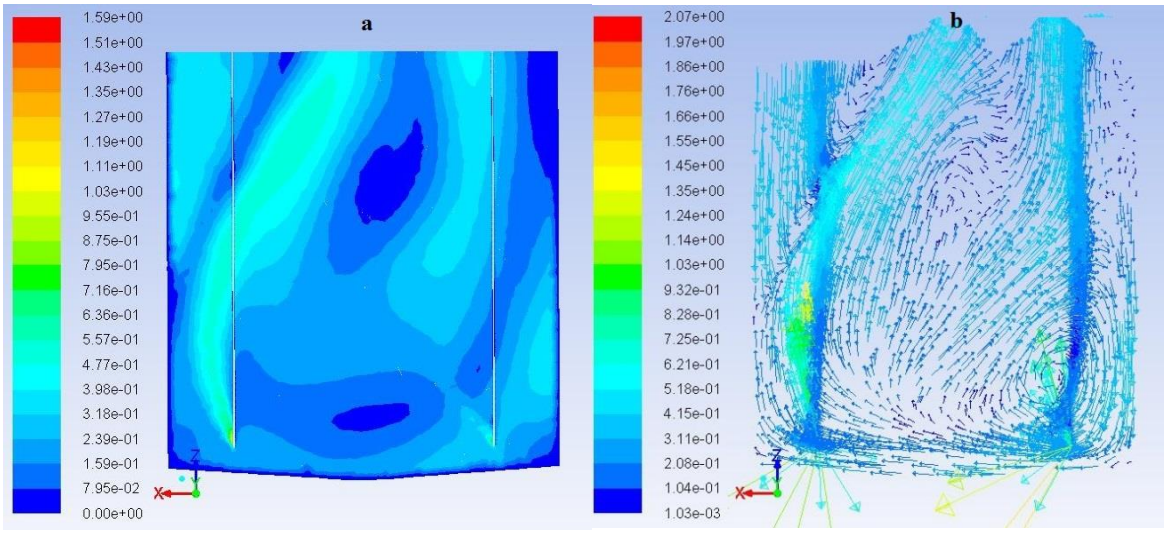

Figure 6-5: a) Liquid velocity profile b) Liquid velocity vectors for 1 mm bubble size after 1800 s of flow time.

6.1.2 5 mm Bubble Size

Development of the liquid velocity profile for 5 mm bubble diameter is shown in Figure 6-6.

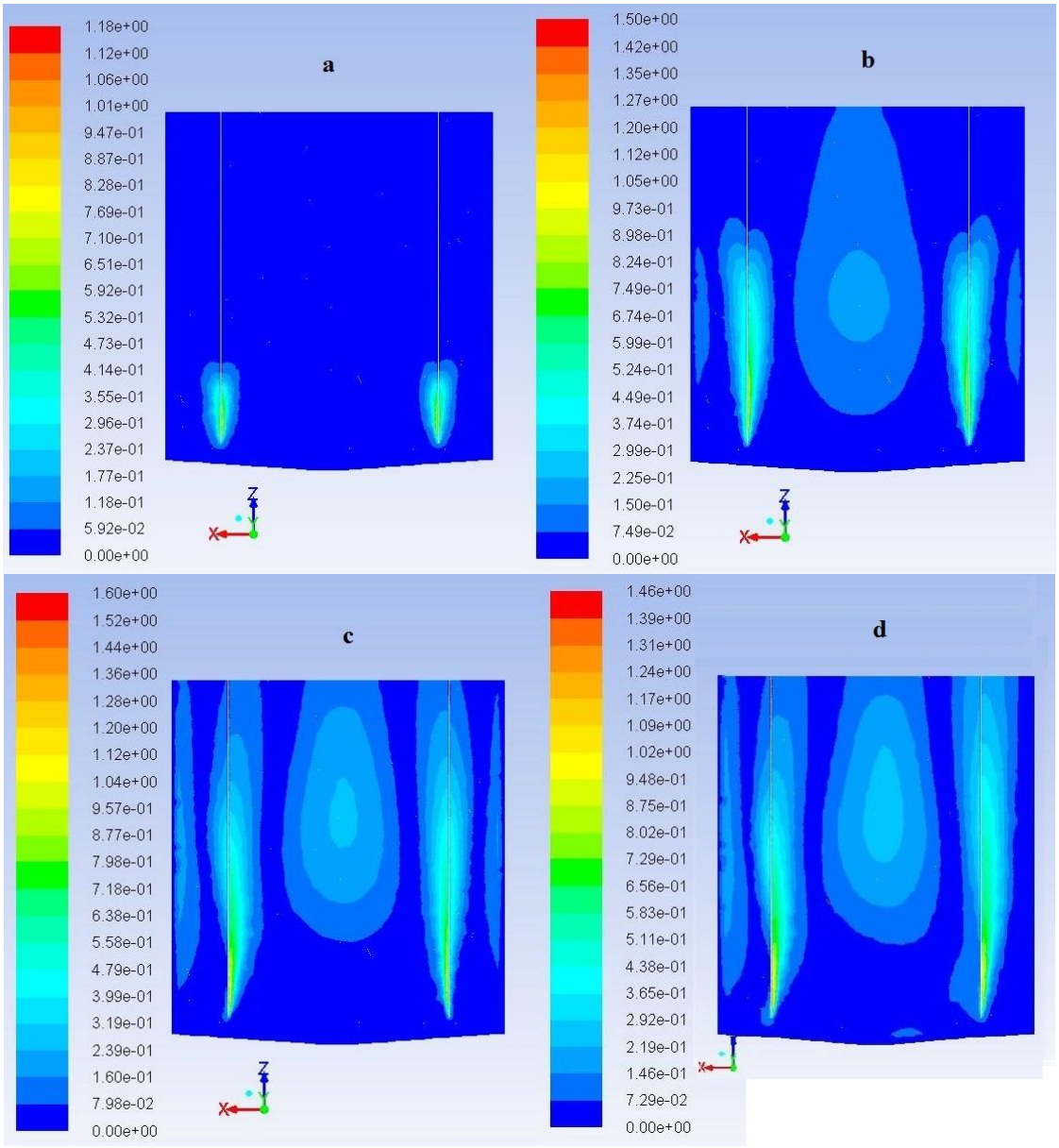

Figure 6-6: Evolution of liquid velocity profile for 5 mm bubble size at a) 30 s b) 100 s c)1800 s d) 3600 s.

Liquid and gas velocity contours of four horizontal planes at different liquid heights of Z=1, 6, 12 and 18 m are illustrated in Figure 6-7 while liquid velocity distribution across the tank diameter at different liquid levels is presented in Figure 6-8.

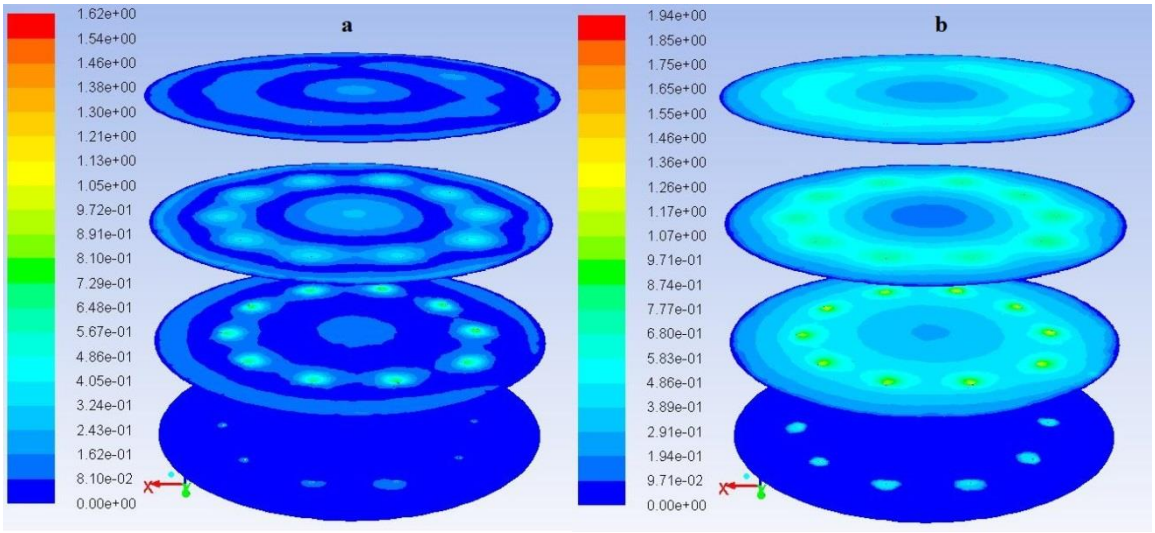

Figure 6-7: a) Liquid velocity b) Gas velocity contours at Z=1, 6, 12, 18 m planes for 5 mm bubble size after 3600 s of flow time.

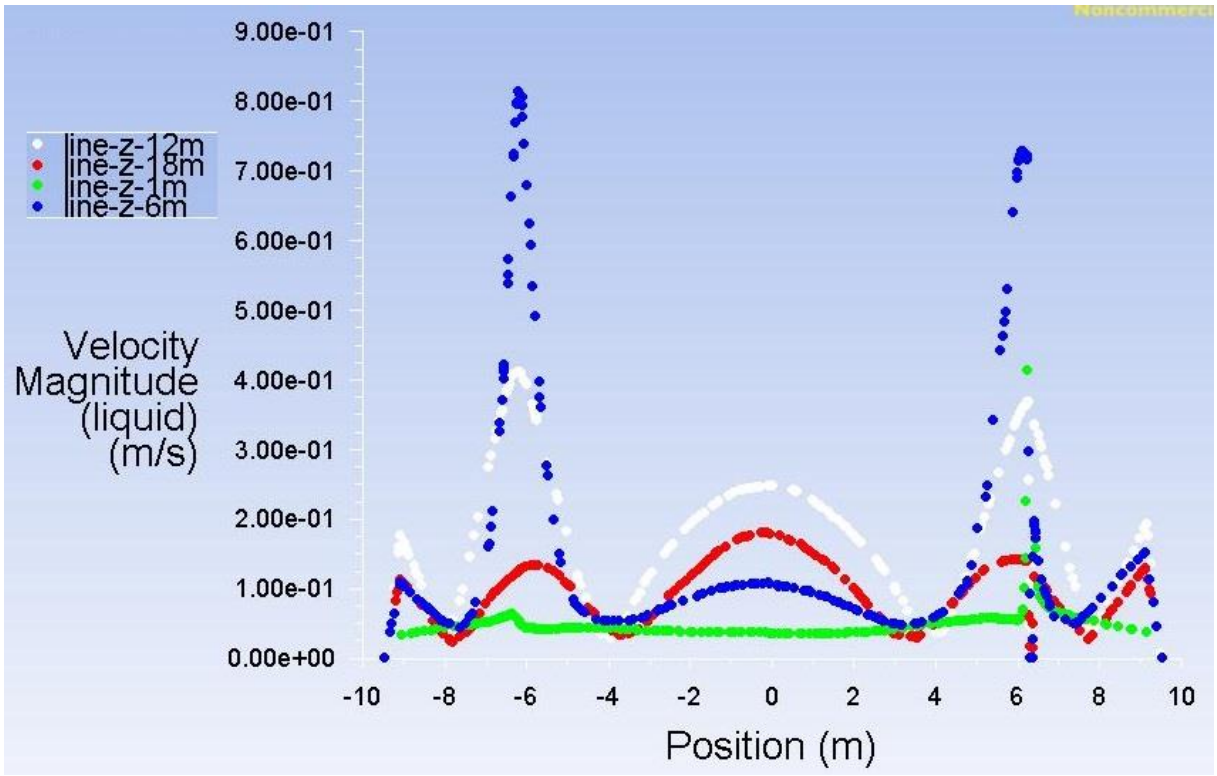

Figure 6-8: Liquid velocity distribution across the diameter of the tank at Z= 1, 6, 12, 18 m for 5 mm bubble size after 3600 s of flow time.

Liquid velocity contour and liquid velocity vector profile was also obtained at the end of the simulation and presented in Figure 6-9 in order to observe the liquid flow distribution across the tank volume and to identify the liquid flow directions and liquid recirculation zones.

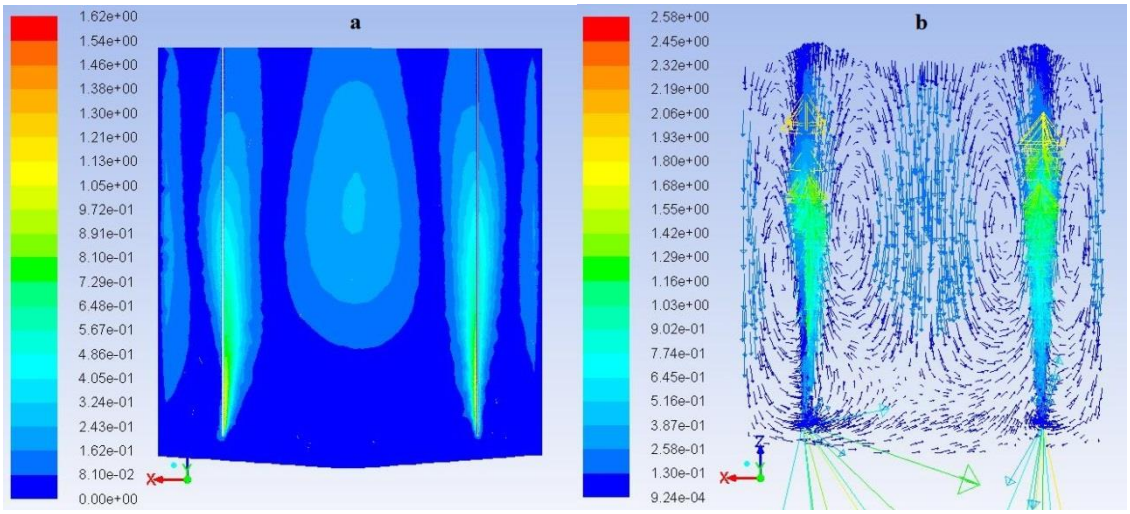

Figure 6-9: a) Liquid velocity profile b) Liquid velocity vectors for 5 mm bubble size after 3600s of flow time

6.1.3 10 mm Bubble Size

Progression of the liquid velocity profile over a period corresponding to 1 hour of flow time is observed and some of the important stages are shown in Figure 6-10.

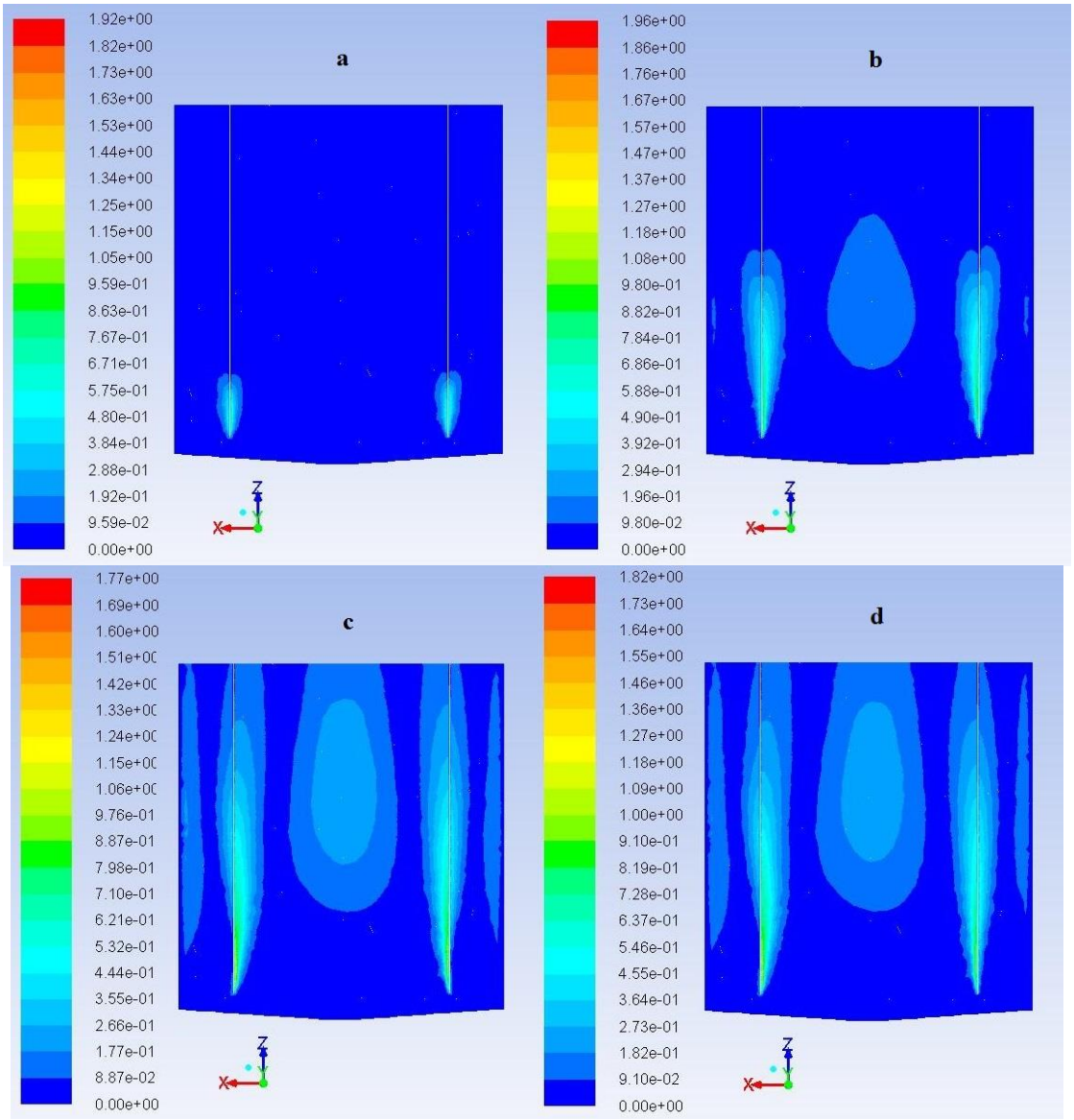

Figure 6-10: Evolution of velocity profile for 10 mm bubble size at a) 25 s b) 85 s c) 1825 s d) 3625 s.

Liquid and gas velocity contours obtained at different horizontal planes similar to other two cases are illustrated in Figure 6-11. Liquid velocity distribution across the tank diameter at different liquid levels is plotted against the X direction which is shown in Figure 6-12. In addition, liquid velocity contour and liquid velocity vector profile obtained at the end of the simulation are presented in Figure 6-13.

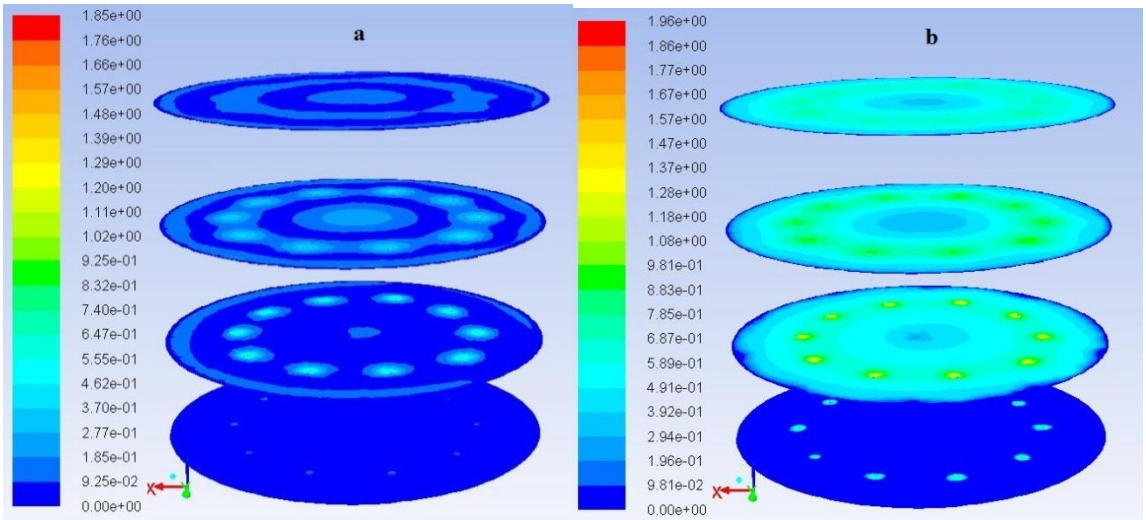

Figure 6-11: a) Liquid velocity b) Gas velocity contours at Z=1, 6, 12, 18 m planes for 10 mm bubble size after 3625 s of flow time.

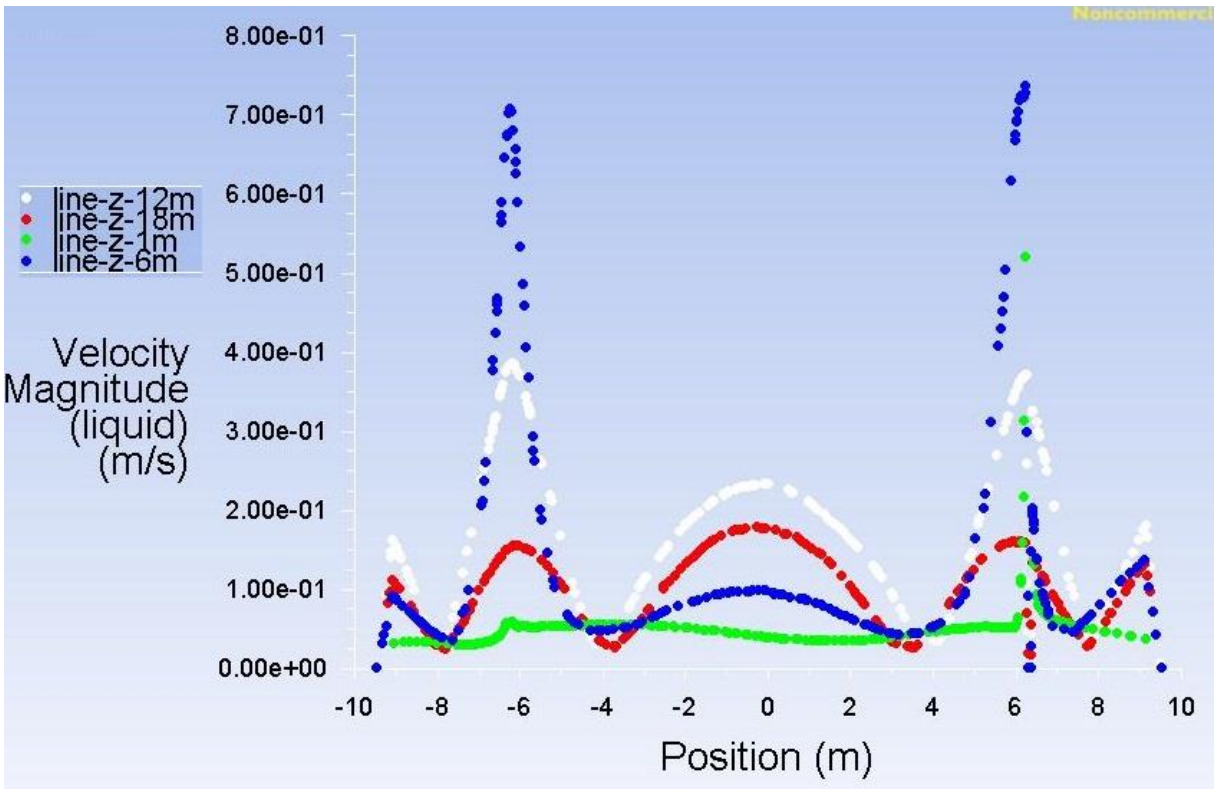

Figure 6-12: Liquid velocity distribution across the diameter of the tank at Z= 1, 6, 12, 18 m for 10 mm bubble size after 3625 s of flow time.

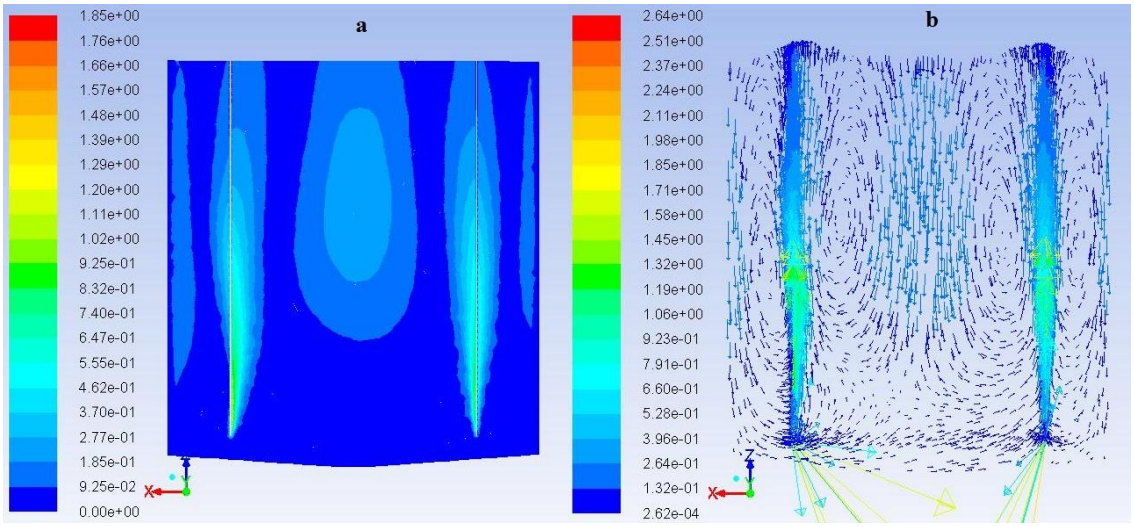

Figure 6-13: a) Liquid velocity profile b) Liquid velocity vectors for 10 mm bubble size after 3625 s of flow time.

6.2 Effect of Inlet Gas Velocity

Figure 6-14 compares the liquid flow fields obtained during 0.6 m/s inlet gas velocity case with the flow fields corresponding to 1.2 m/s inlet gas velocity case for 5 mm bubble size and initial gas flow arrangement. Both cases have simulated for about 1 hour of flow time.

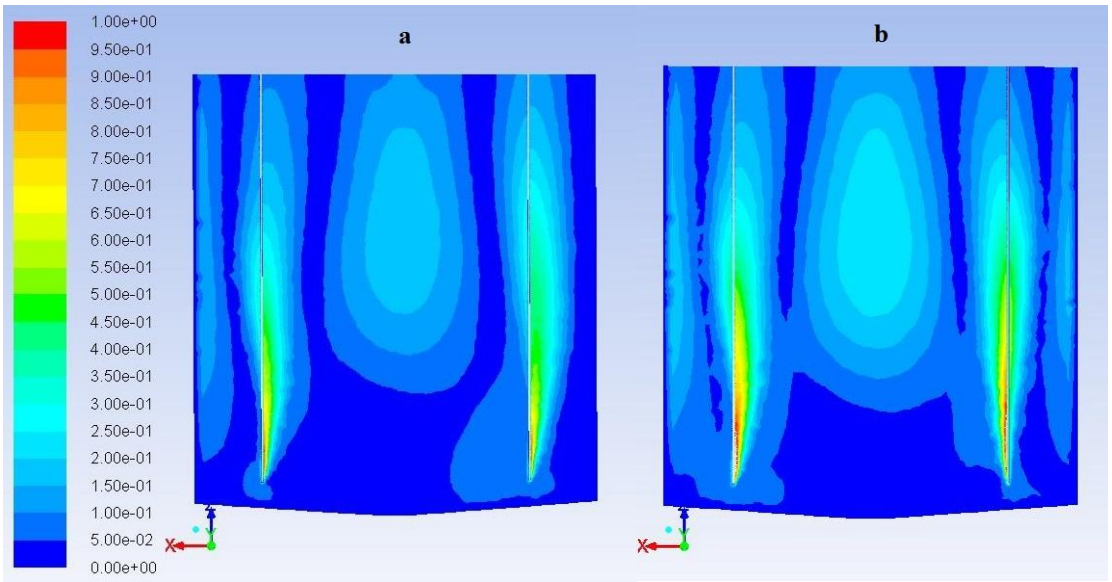

Figure 6-14: Comparison of liquid velocity profiles of a) 0.6 m/s b) 1.2 m/s inlet gas velocity for 5 mm bubble size after 3600 s of flow time.

Final liquid velocity profiles obtained at different horizontal planes for 0.6 m/s inlet gas velocity case are compared with the 1.2 m/s case in Figure 6-15. Liquid velocity vector profiles of both cases are compared in Figure 6-16.

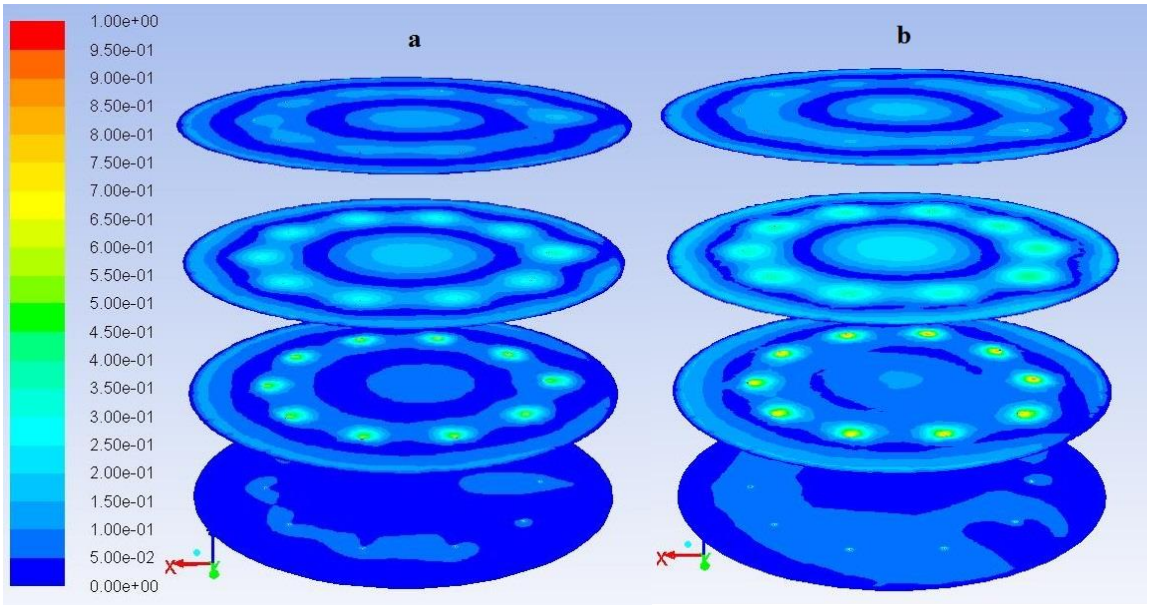

Figure 6-15: Comparison of liquid velocity profiles of a) 0.6 m/s b) 1.2 m/s inlet gas velocity at horizontal planes for 5 mm bubble size after 3600 s of flow time.

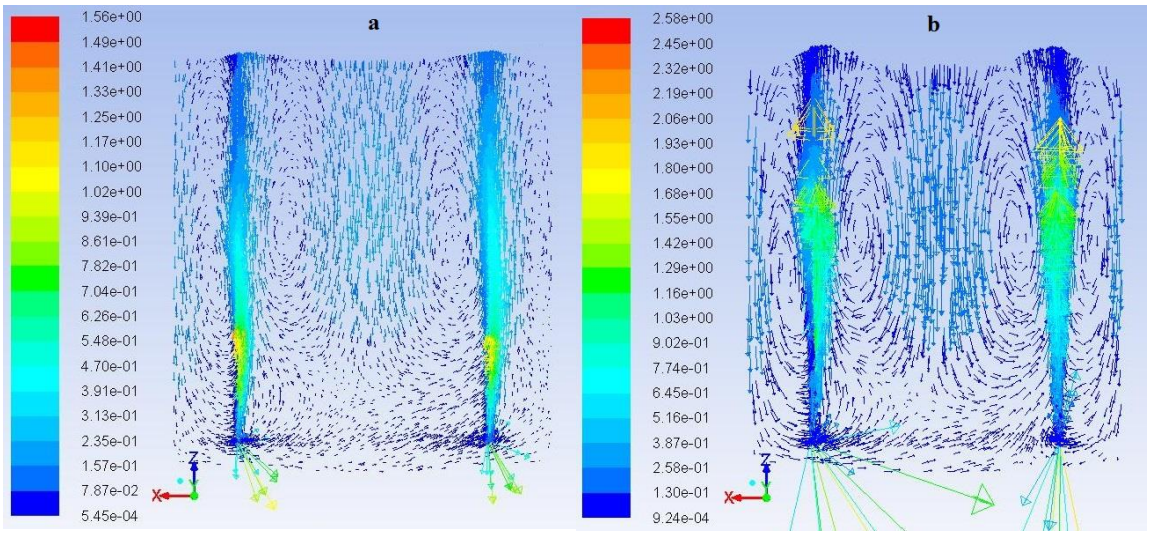

Figure 6-16: Comparison of liquid velocity vectors of a) 0.6 m/s b) 1.2 m/s inlet gas velocity for 5 mm bubble size after 3600 s of flow time.

6.3 Effect of Source Term

Source term was added to the biogas phase after the solution reached to a stable state (after 1300s of flow time) in order to facilitate faster convergence. Then the simulations have run till 1 hour of flow time to compare the results with the case without the source term. A comparison liquid velocity profiles obtained with and without the inclusion of source term is shown in Figure 6-17.

Liquid velocity profiles captured at different horizontal planes inside the reactor are compared in Figure 6-18.

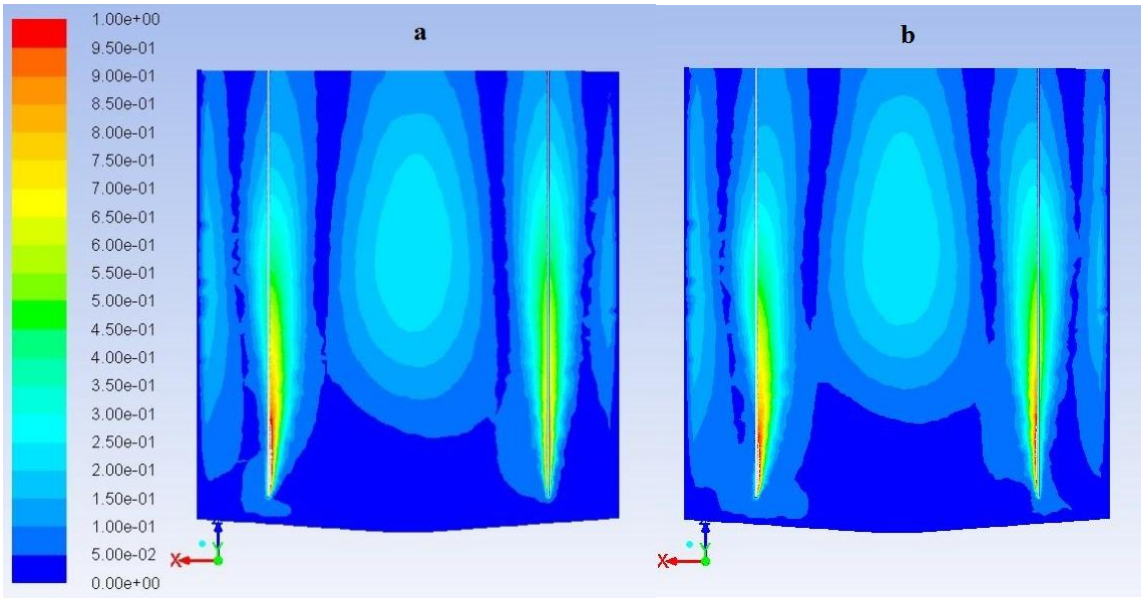

Figure 6-17: Comparison of liquid velocity profiles a) with source term b) without source term for 5 mm bubble size after 3600 s of flow time.

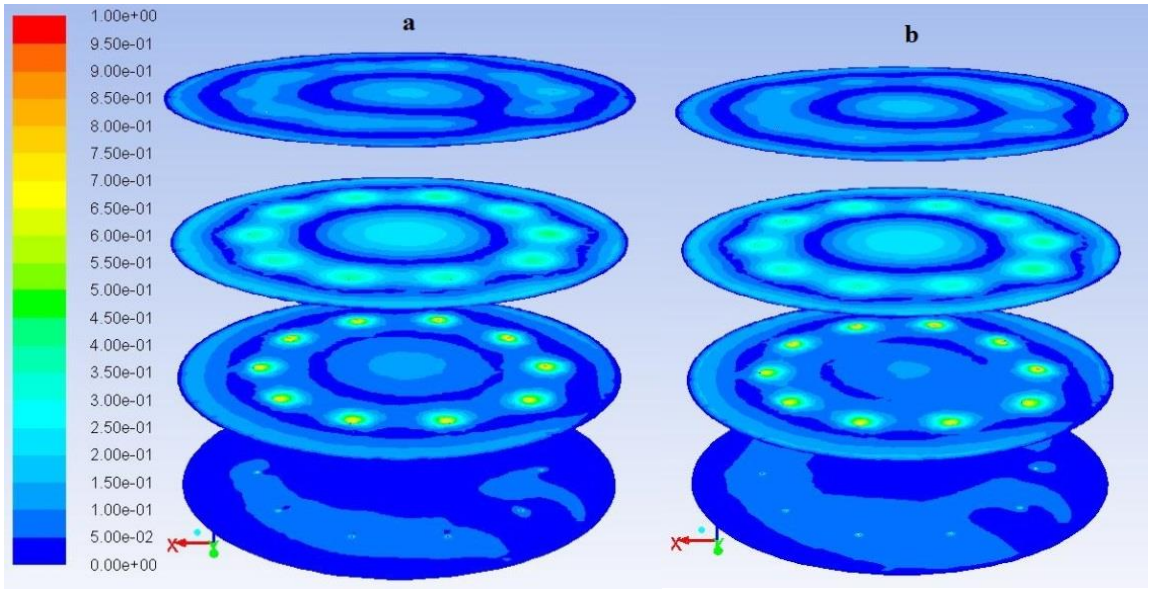

Figure 6-18: Comparison of liquid velocity profiles a) with source term b) without source term at horizontal planes for 5 mm bubble size after 3600 s of flow time.

Gas velocity profiles of both cases are compared after running the simulations for a similar period of time which are shown in Figure 6-19. Figure 6-20 compares the gas phase volume fractions with and without the addition of source term.

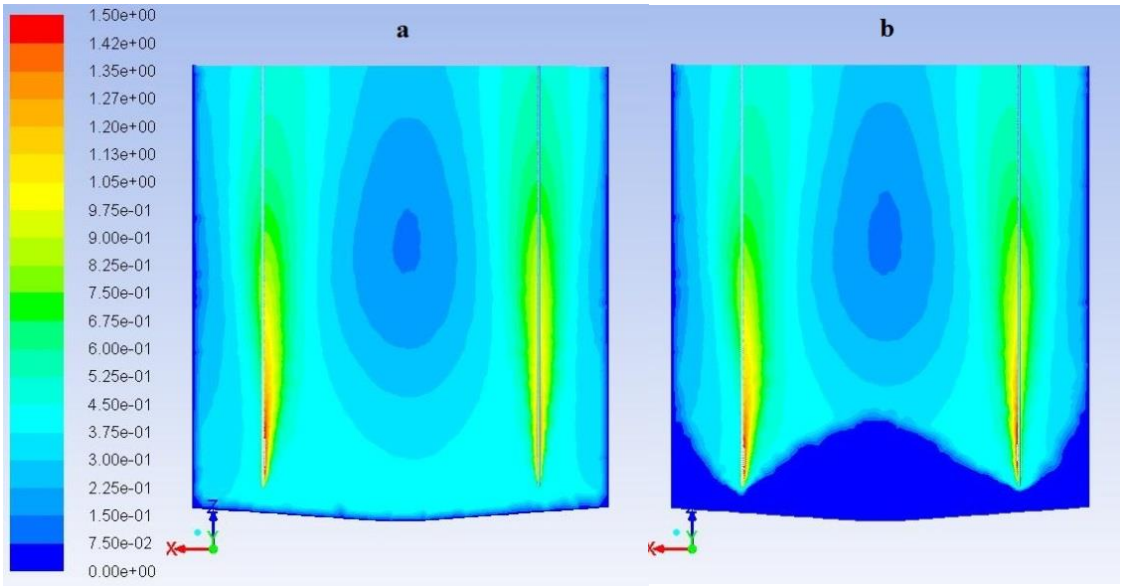

Figure 6-19: Comparison of gas velocity profiles a) with source term b) without source term for 5 mm bubble size after 3600 s of flow time.

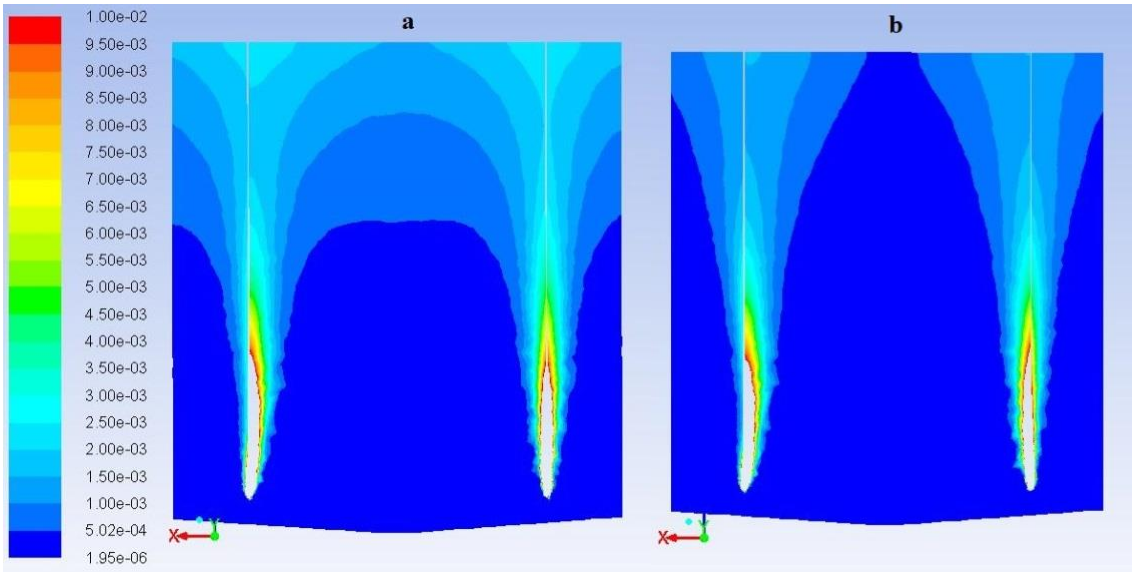

Figure 6-20: Comparison of gas phase volume fraction a) with source term b) without source term for 5 mm bubble size after 3600 s of flow time.

6.4 Effect of Gas Distribution Arrangement

Initially velocity inlet 1 was used to distribute the gas at a velocity of 2.4 m/s for 900 s (15 minutes). Then the gas flow was paused for around 60 s and then velocity inlet 2 was used to distribute the gas for another 900 s. The evolution of the liquid velocity profiles throughout the whole cycle is presented in Figure 6-21.

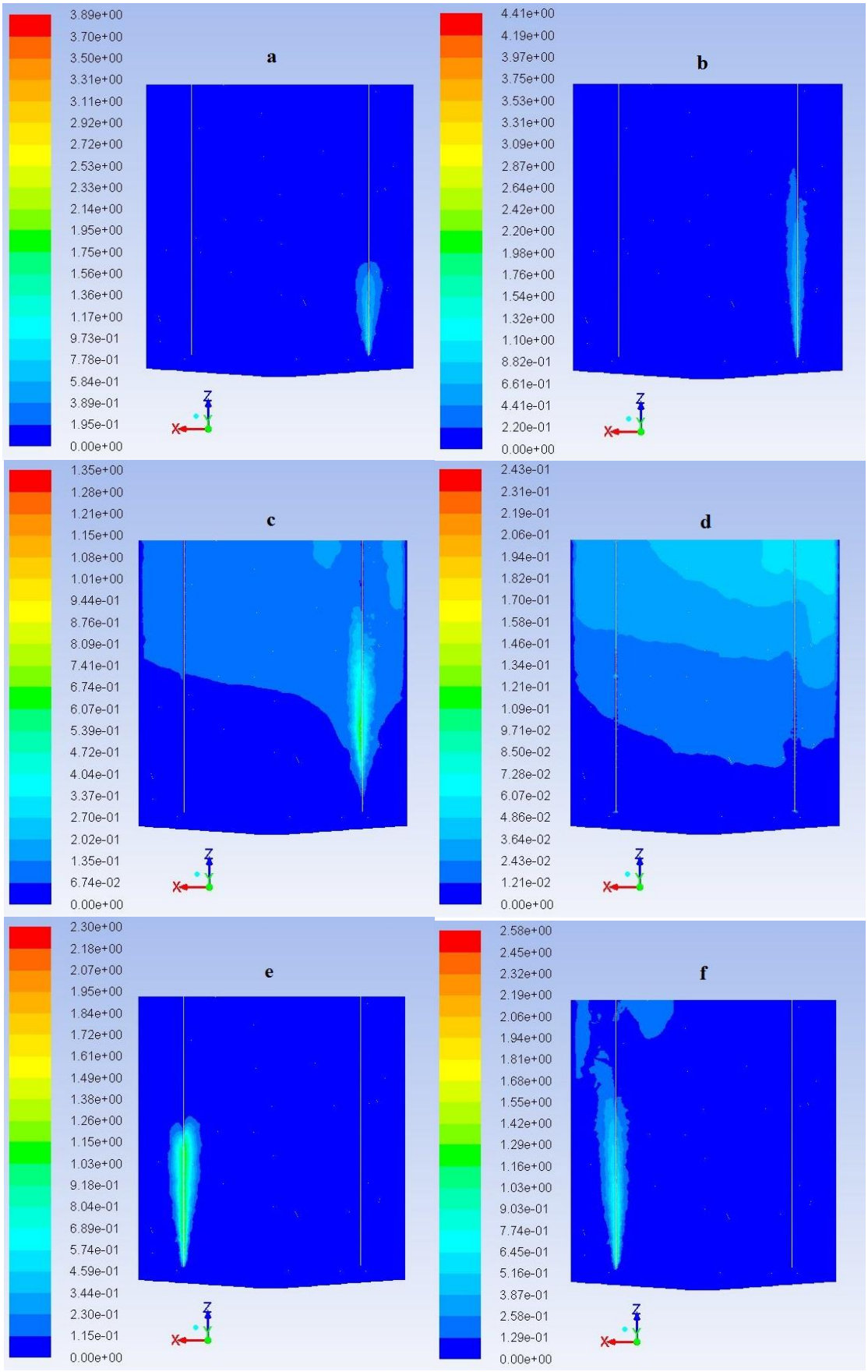

Figure 6-21: Evolution of velocity profiles for 10 mm bubble size at a) 30 s b) 885 s c) 910 s d) 966 s e) 980 s f) 1860 s for existing gas distribution arrangement.

A comparison of the liquid velocity fields of Y=0 plane at the end of each stage (i.e. at 900 s, 960s and 1860 s) is presented in Figure 6-22. Figure 6-23 compares the velocity contours of horizontal planes inside the liquid volume. Same velocity scale is used for all the comparisons by setting maximum velocity to 1 m/s while plotting the contours.

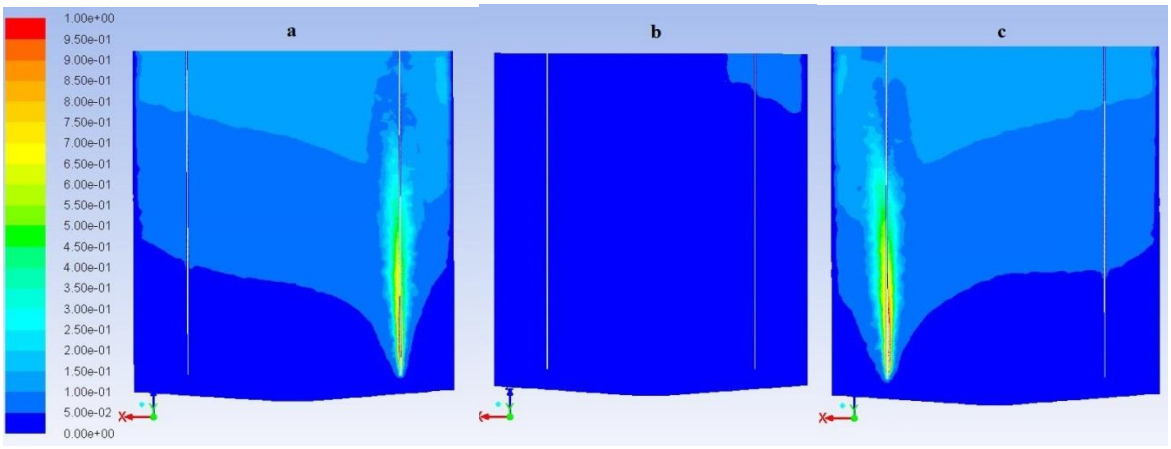

Figure 6-22: Comparison of liquid velocity profiles at a) 900 s b) 960 s c) 1860 s for 10 mm bubble size.

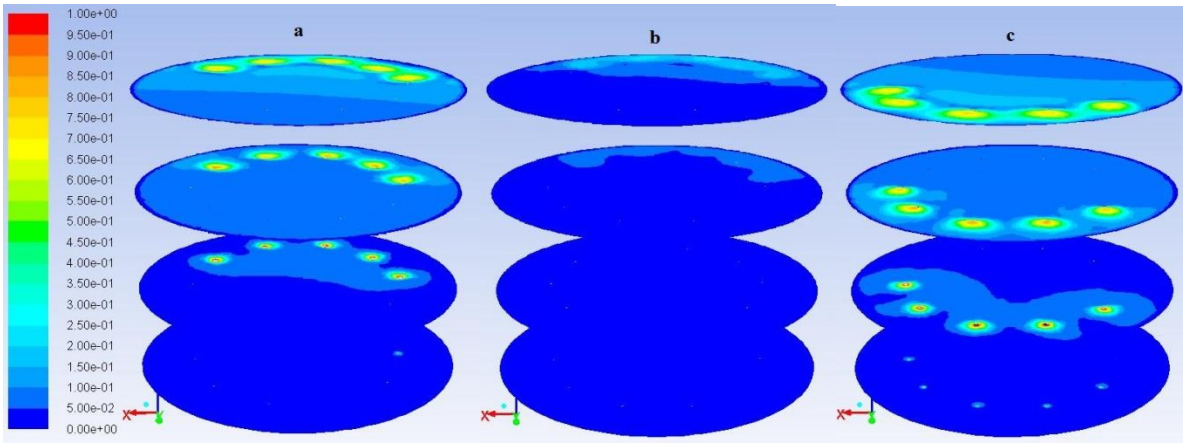

Figure 6-23: Comparison of liquid velocity profiles at a) 900 s b) 960 s c) 1860 s at horizontal planes for 10 mm bubble size.

Apart from the velocity profiles, velocity vectors were also analyzed to get an overview of the liquid recirculation directions at different stages of the process. Figure 6-24 illustrates the liquid velocity vectors of Y=0 plane at 900 s, 960 s and 1860 s time intervals respectively.

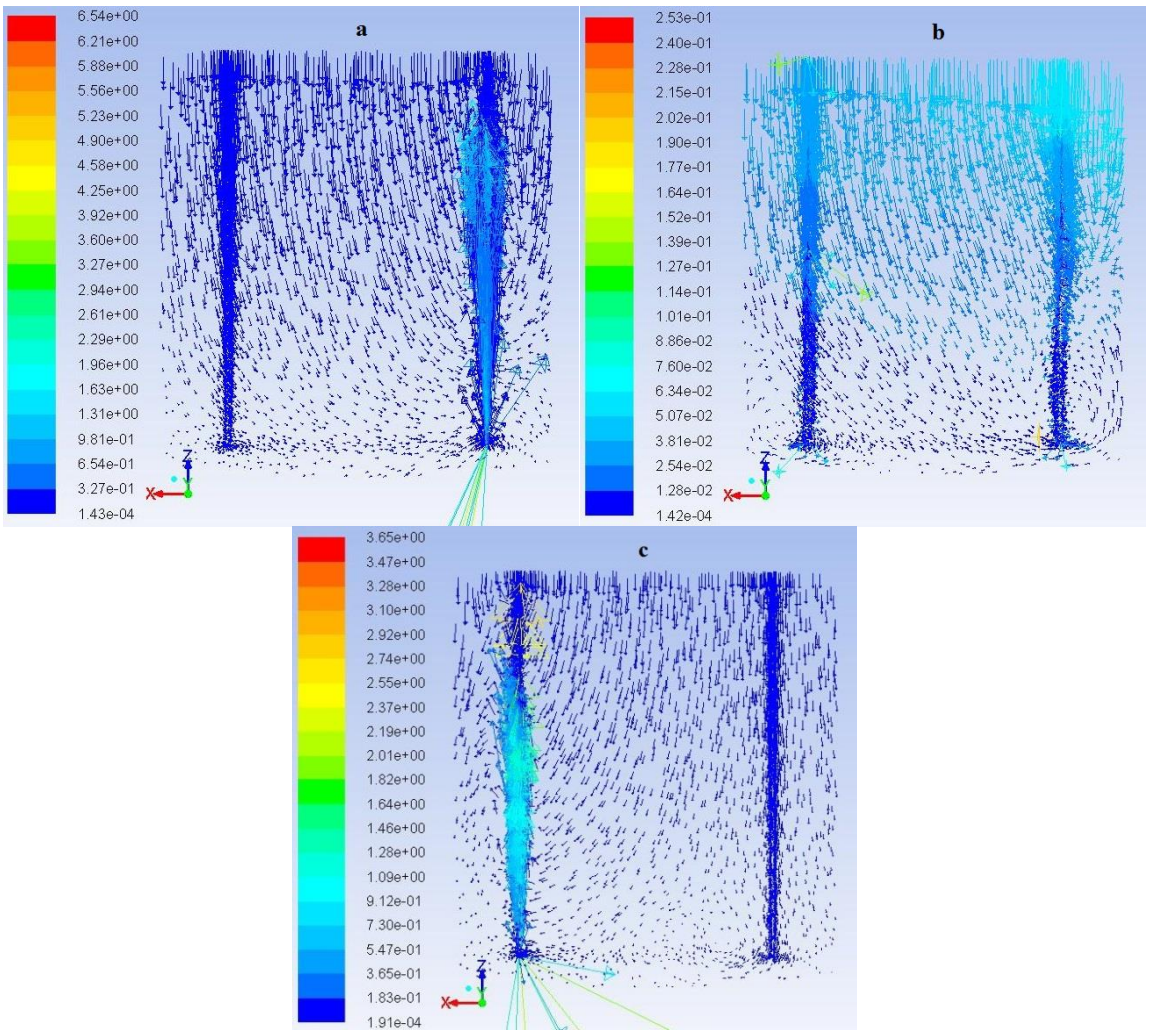

Figure 6-24: Comparison of liquid velocity vectors at a) 900 s b) 960 s c) 1860 s for 10 mm bubble size.

Variation of liquid velocity magnitude across the diameter of the tank along B-B line (Figure 6-25) at different liquid levels of the reactor is shown as XY plots in Figure 6-26.

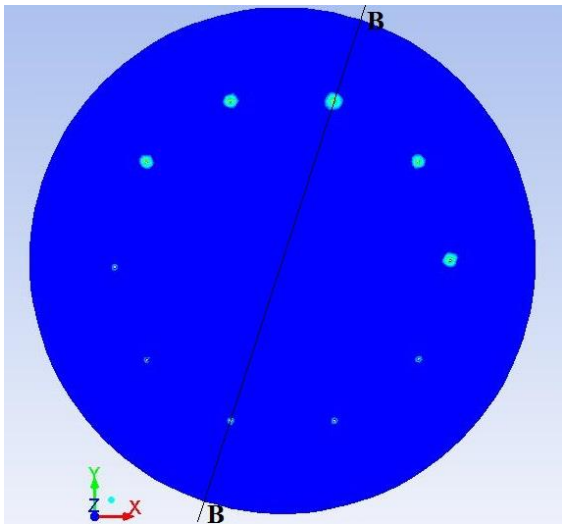

Figure 6-25: B-B line across which the XY plots of velocity magnitudes were obtained.

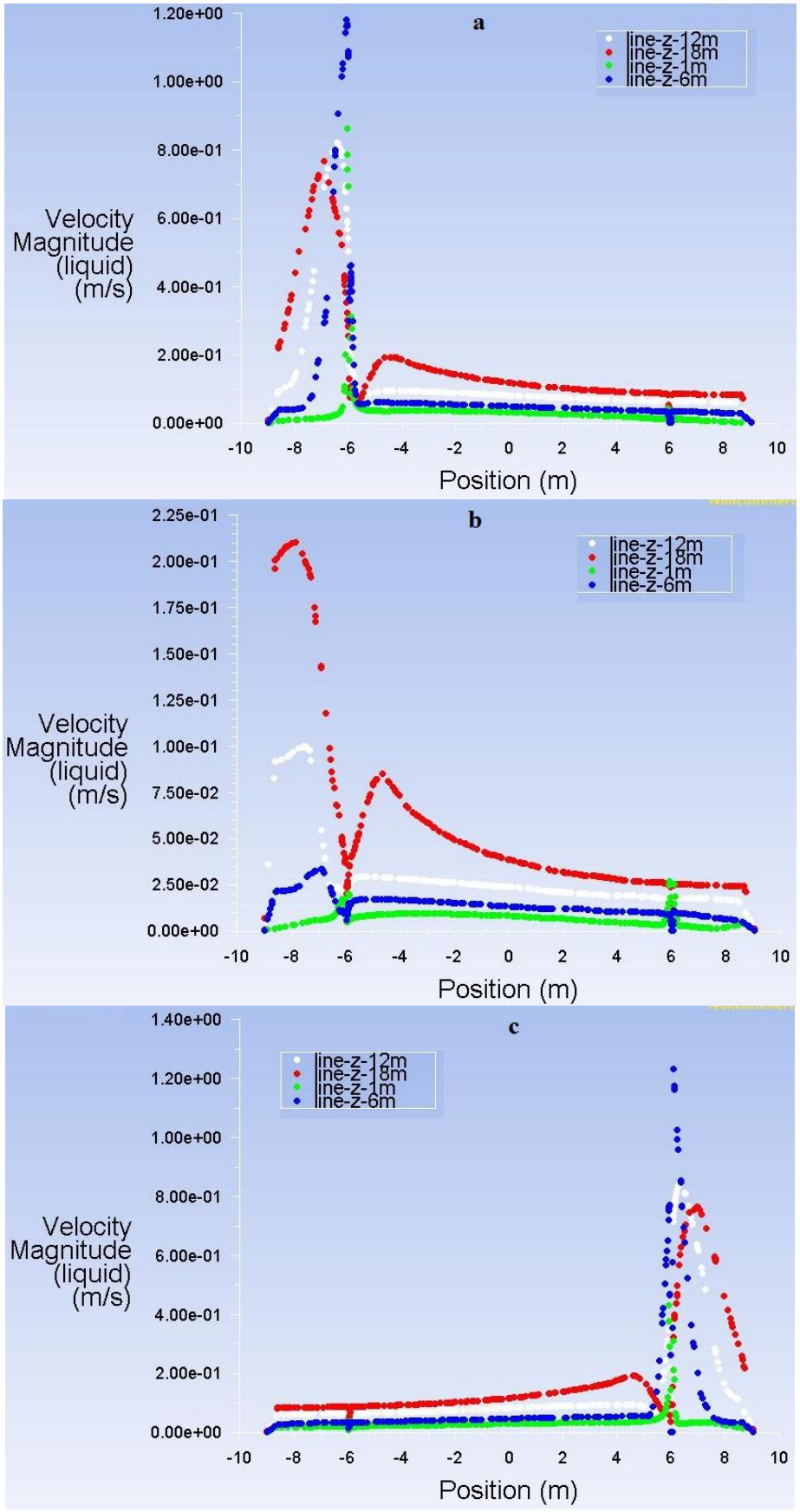

Figure 6-26: Comparison of liquid velocity distribution across the diameter of the tank at a) 900 s b) 960 s c) 1860 s for 5 mm bubble size.

7 Discussions

CFD simulations were performed to investigate the gas and liquid flow characteristics inside a biogas reactor at VEAS. The influence of the boundary conditions and other parameters such as gas bubble size, gas inlet velocity, gas distribution arrangement and presence of a source term, on the hydrodynamics of the reactor was also examined.

7.1 Effect of Gas Bubble Size

Three gas bubble sizes of 1 mm, 5 mm and 10 mm were used during the simulations. All the cases except for the last case were carried out with the initial gas distribution arrangement (i.e. 10 gas outlets operating at the same time) and inlet gas velocity of 1.2 m/s.

1 mm bubble size demonstrated quite dissimilar gas and liquid flow fields compared to the other two bubble sizes. The velocity contours at Y=0 plane of both liquid and gas has shown a symmetrical behavior until the solution reach 200 s of flow time. But with the progression of the solution, drastic changes in the flow patterns were observed as shown in Figure 6-2. The system took considerably long time to converge at each time step compared to two other cases, probably due to the smaller size of the gas bubbles. Therefore, the simulations were carried out only until 30 minutes of flow time to save computational time and resources. By observing the flow patterns of the horizontal and vertical cross sections of the tank in Figure 6-3 and Figure 6-5, it is apparent that the velocity distribution is quite good inside the liquid volume. Liquid velocity vectors obtained at the end of the simulation also display a rigorous and uneven liquid circulation pattern in Figure 6-5. Liquid velocity distribution across the diameter of the tank at different liquid heights (i.e. Z=1, 6, 12, 18 m) which is shown in Figure 6-4 doesn't display any significant pattern.

In contrast to the 1mm bubble size case, 5 mm bubble size case exhibited a good stability during the simulation process. The evolution of the liquid flow pattern is shown in the Figure 6-6 with 4 snapshots of liquid velocity contours at different stages of the simulation during 1 hour of flow time. It can be observed from the Figure 6-7 and Figure 6-9 that the flow patterns demonstrate symmetry in both horizontal and vertical planes of the reactor. Both liquid and gas velocity profiles reached into a stable state after 1800 s of flow time. As illustrated in Figure 6-7, the liquid and gas velocities appear to be higher at the center of the tank and lower at the top and bottom sections. Some low velocity zones (below 0.08 m/s) can be identified between the bottom of the tank and gas inlets, between pipes and tank wall and at an annular liquid volume between central axis of the tank and pipes. Velocity distribution profiles across the tank diameter provide a good overview of the liquid and gas velocity values in the tank. From the XY plot in Figure 6-8, it can be noted that the liquid and gas velocities have higher values around the pipes and at the center of the tank. A proper liquid recirculation can also be noticed from the liquid velocity vectors in Figure 6-9.

10 mm bubble size case displayed similar flow patterns as the 5 mm bubble size. In some occasions, the simulations converged even faster than the 5 mm case. Liquid velocity profiles reached to a stable state within 1650 s of flow time and the velocity contours were almost symmetric in both horizontal and vertical planes as shown in Figure 6-10 and Figure 6-11. Low velocity zones below 0.09 m/s of liquid velocity can be observed in the similar areas as 5 mm bubble size case. XY plots across the tank diameter have shown identical trends as presented in Figure 6-12.

Liquid velocity profiles of all the three bubble sizes were compared in Figure 7-1 and Figure 7-2. According to the figures, liquid velocity characteristics of both 5 mm and 10 mm bubble size cases demonstrate similar symmetric behavior while 1 mm bubble size shows an irregular flow pattern. But it can be seen than the velocity distribution in 1 mm case is comparatively better than two other cases with higher velocity throughout the liquid volume.

Considering the velocity profiles in the horizontal planes, 5 mm case shows relatively higher velocity than 10 mm case in Z=1 m and Z=6 m planes.

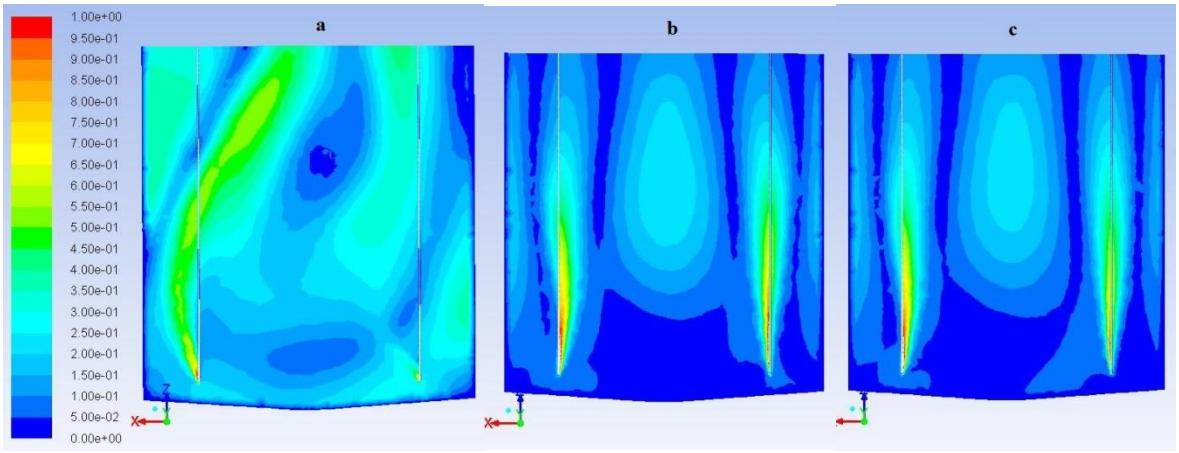

Figure 7-1: Comparison of liquid velocity profiles for a) 1 mm b) 5 mm c) 10 mm bubble sizes at the end of the simulation.

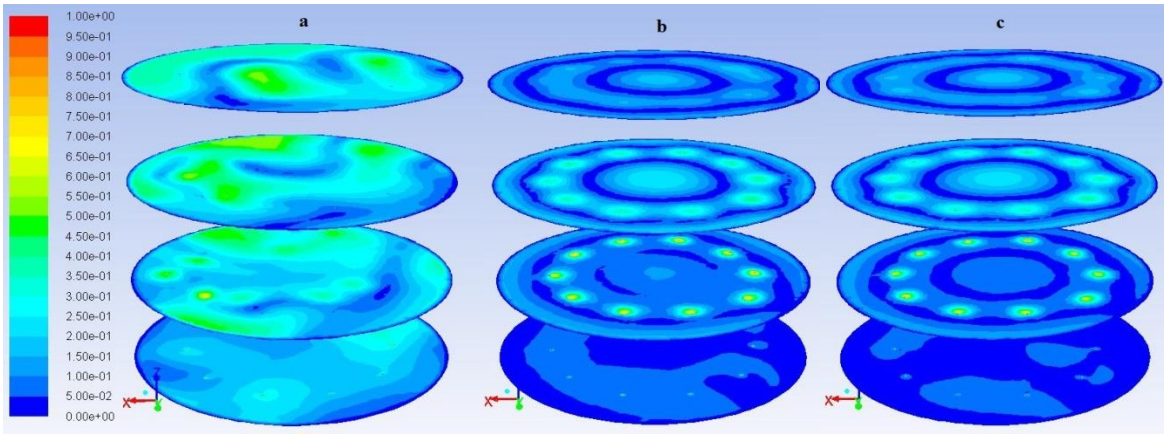

Figure 7-2: Comparison of liquid velocity profiles for a) 1 mm b) 5 mm c) 10 mm bubble sizes at horizontal planes at the end of the simulation.

Given the fact that the diameter of the pipes which produce bubbles inside the tank are quite larger compared to the typical hole diameter of a common bubble columns in previous studies[4, 12], 5 and 10 mm bubble diameters will provide reasonable results for the simulations in this study.

All the simulations in this study were performed with a single characteristic bubble size at a given time. But the actual process generally involves a bubble size distribution which will make the simulation process very complex as each bubble size must be treated as a separate phase. In addition, the assumption of the single bubble size will neglect the effects bubble coalescence and break-up inside the reactor.

Terminal velocity and rise time of a gas bubble are two important factors when it comes to gas bubbling processes in liquid. Velocity of the bubbles affects the liquid velocity while the bubble rise time decides how long the liquid will maintain its turbulence after the bubbling process stops. Therefore, the terminal velocity and the rise time of different bubble sizes were calculated and plotted in Figure 7-3 to compare the results. The calculations are presented in Appendix D.

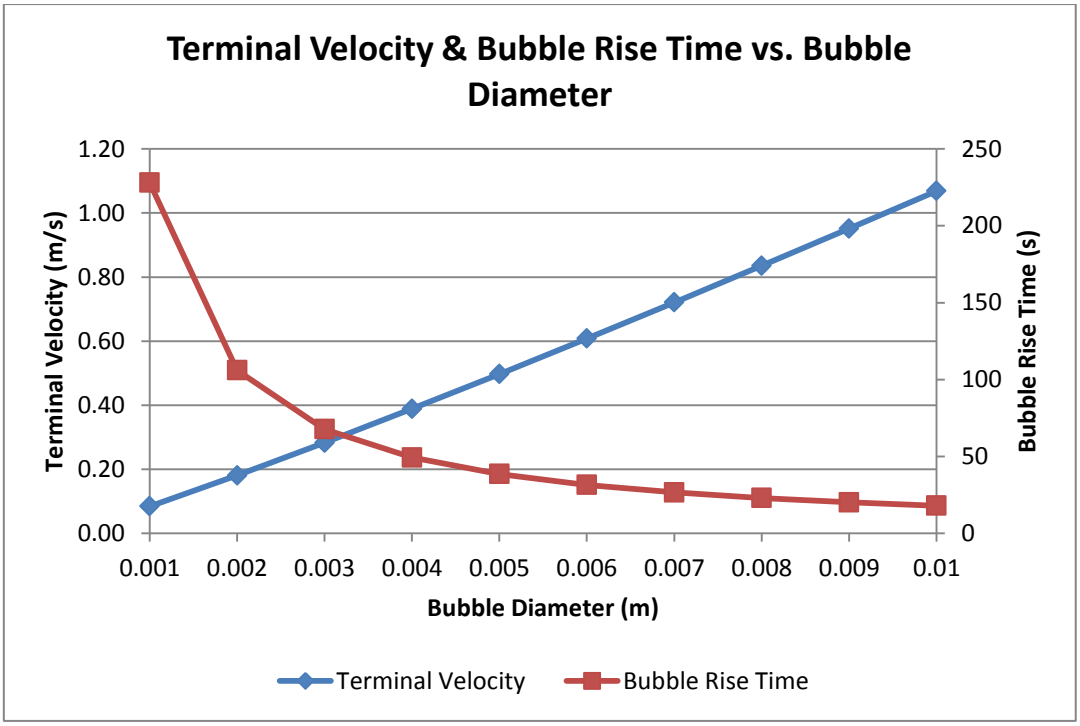

Figure 7-3: Variation of terminal velocity and rise time of a gas bubble with bubble size.

From the plot, it can be observed that the terminal velocity increases linearly with the bubble size while the bubble rise time exhibit a sort of exponential decay. The smallest bubbles (1mm) will take around 4 minutes to escape from the liquid while largest bubbles will leave the liquid within around 20 seconds. The haphazard flow patterns of the 1 mm bubble size can be described with the bubble rise time inside the reactor. The smaller bubbles will tend to decrease the average fluid density because they take longer time to reach the liquid surface

and hence reduce the buoyancy of the system. This will cause the liquid and gas inside the reactor susceptible to chaotic fluctuations thus causing irregular flow patterns.

7.2 Effect of Inlet Gas Velocity

During the simulations, different inlet gas velocities were used at the velocity inlets depending on the case. Initially 1.2 m/s of inlet velocity was used with 10 pipe gas distribution arrangement. Then an inlet velocity of 0.6 m/s was used with the same arrangement to compare the results.

The liquid velocity profile of the 0.6 m/s case observed to be stabilized within 1170 s of flow time which was considerably low compared to the 1.2 m/s case which took around 1800 s to reach a stable state.

According to liquid velocity profile comparison in Figure 6-14 and Figure 6-15, 1.2 m/s inlet velocity case demonstrate a wider distribution of liquid velocity both in the vertical plane and horizontal planes. 0.6 m/s inlet velocity case have larger area low velocity zone of which the liquid velocity is below 0.01 m/s compared to the original case of 1.2 m/s inlet velocity.

According to the Figure 6-16, the liquid velocity vector profile in 0.6 m/s gas velocity case shows two main liquid recirculation zones at the middle of the tank close to the pipes. But, in the initial case of 1.2 m/s inlet gas velocity, four noticeable liquid recirculation zones can be identified. Two of these recirculation zones locate between tank wall and the pipes which provide better liquid mixing in that region. In addition, a downward flow of the bulk liquid can be observed around the central axis of the tank with a comparably higher velocity than most of the other regions in the tank.

During the simulations with the actual gas distribution arrangement, gas inlet velocity of 2.4 m/s was used as it only employed 5 pipes at a time with the same gas flow rate of 300 Nm^3/h. While one velocity inlet (i.e. 5 pipes) operated with 2.4 m/s velocity, other velocity inlet kept at 0 m/s velocity. This will be further discussed in a subsequent section of this report.

7.3 Effect of Source Term

Generation of biogas during the AD process will contribute to an extra amount of gas phase inside the reactor. According to some literature, this could also contribute to the liquid mixing[4]. Therefore, a comparison is carried out for the 5 mm bubble size with and without the source term. Since addition of the source term from the beginning of the simulation caused stability problems, it was decided to add it after the solution reached a reasonable stability. The simulations were performed until 1 hour of flow time and compared with the case without the source term.

From the liquid velocity contours illustrated Figure 6-17and Figure 6-18, it is obvious that the addition of source term has caused a very little or no change to the liquid velocity characteristics of the original case. In contrast, the gas velocity contours demonstrates a clear difference between the two cases as shown in Figure 6-19. The gas velocity seems to be distributed across the whole liquid volume after the addition of the source term. A development of the gas phase volume fraction can be observed especially in the middle of the tank with the increase of liquid height as seen in Figure 6-20.

7.4 Effect of Gas Distribution Arrangement

Initially the velocity inlet 1 was used to distribute gas inside the reactor for 15 minutes. During the simulations, it was observed that the simulations took longer time to converge than the previous gas distribution arrangement which employed all the 10 pipes. From the Figure 6-21, it is apparent that a high velocity zone has developed around the pipes. The velocity profiles eventually have reached to a stable state within 860 s. The velocity at the bottom of the tank on the opposite side of the inlets observed to be very low compared to the other areas.

After running the simulation for 15 minutes, the gas distribution has stopped similar to the actual process at VEAS. But it was noticed that the simulations take very long time to converge when the gas flow has stopped. Therefore, the simulations had to be restricted to 60 s of flow time after the pause as it took more than 7 days of computational time to reach to that stage. Even after 60 s of pause, the liquid velocity of the entire tank dropped below 0.05 m/s which can be observed in Figure 6-22.

Then velocity inlet 2 has been employed to distribute gas for another 15 minutes (until 1860 s of total flow time). Simulations were begun at smaller time steps and increased gradually to achieve faster convergence. Development of the velocity profile was almost similar to the opposite side of the tank during the initial 15 minutes of flow time. A close to stable state was achieved around 1810 s of total flow time.

Figure 6-22 and Figure 6-23 compare the liquid velocity contours at three main stages of the process. It can be observed from Figure 6-22 that approximately one third of the tank's velocity is below 0.05 m/s even after 900 s and 1860 s where fully developed flow field is expected. According to Figure 6-23, it is evident that the liquid velocity at the top part of the tank is higher than the rest of the liquid volume. This can also be justified by the XY plots across the tank diameter as shown in Figure 6-26. This particular behavior is quite different from all the other case in this study where higher liquid velocity was observed at the middle part (i.e. between 8 m – 12 m liquid height) of the tank.

Liquid recirculation patterns are as important as liquid velocity magnitudes to evaluate the performance of the mixing inside the biogas reactor. Figure 6-24 illustrates the liquid velocity vector profiles at 900 s, 960 s and 1860 s, the three main stages of this process. It can be

observed that a bulk downward liquid motion takes place towards the operating gas inlets while an upward motion of liquid can be noticed close to the gas pipes. Very small liquid recirculation zones can also be observed close to the pipes. It will be quite interesting compare the liquid recirculation patterns of new gas distribution arrangement with the previous 10 pipes gas distribution system.

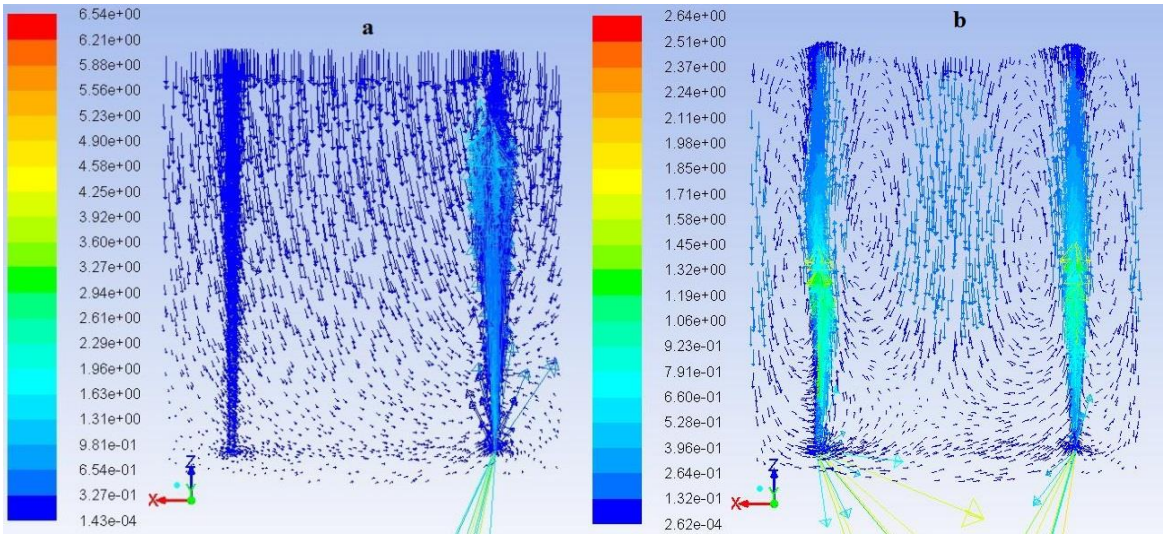

Figure 7-4: Comparison of liquid velocity vectors of a) new b) initial gas distribution arrangements for 10 mm bubble size after stabilization of the flow.

From Figure 7-4, a significant difference of the liquid recirculation patterns between the two gas distribution arrangements can be identified. The initial gas distribution arrangement seems to have couple of prominent liquid recirculation zones in the middle part of the tank compared to the existing gas distribution system at VEAS. Hence, this may eventually promote the liquid mixing inside the reactor and can be recommended to apply instead of the existing arrangement.

During this case of study, gas velocity of the corresponding inlet is set to zero to indicate the pause of the flow. This can also be achieved by setting the particular inlet as a wall for the required occasion. As both of these methods provides same results, the first method was adopted for the whole process.

8 Conclusion

Anaerobic digestion is considered as one of the promising biological waste treatment methods available at most of the sewage and wastewater treatment plants. AD systems offer multiple benefits such as reduction of greenhouse gasses, generation of electricity and heat from the biogas in addition to its main purpose of waste reduction. The main focus of this study is to investigate the three dimensional gas liquid flow characteristics inside one of the anaerobic digester at VEAS, a large scale sewage treatment plant located at Oslo. CFD simulations have been used to simulate the gas and liquid flow fields in the reactor.

Commercial CFD software, ANSYS FLUENT 13.0 has been used for the simulations and GAMBIT 2.4.6 version, a preprocessor to FLUENT has been used to generate the problem geometry and computational mesh. Initially, the simulations were run with three different gas bubble sizes of 1 mm, 5 mm and 10 mm in order to investigate the influence of gas bubble size on the gas and liquid flow fields. Effect of inlet gas velocity and the generation of biogas inside the reactor on the flow characteristics are also observed with selected bubble sizes. Finally, the actual gas distribution arrangement at VEAS was simulated and compared with the initial gas distribution arrangement in order to provide recommendations to the existing system.

From the simulations with the different bubble sizes, it was observed that both 5 mm and 10 mm bubble sizes demonstrate similar symmetric flow fields while 1 mm bubble size displayed irregular flow fields. In addition, 5 mm bubble diameter displayed a better liquid velocity distribution at different heights of the tank compared to the 10 mm case, even though the difference was not very significant. Considering about the stability of the simulation process, 10 mm bubble size exhibited a faster convergence at each time step compared to two other cases. Therefore, it can be concluded that the 10 mm bubble size will be a reasonable assumption as the average bubble size for this particular study. This can also be justified with the larger diameter (75 mm) of the gas distribution pipes in the biogas reactor.

Using a low inlet gas velocity resulted in a faster stabilization of the liquid flow fields. Velocity contours of 0.6 m/s inlet gas velocity case has reached to a stable state within 1170 s while the initial case of 1.2 m/s inlet gas velocity took around 1800 s to achieve stable flow patterns. But high inlet gas velocity case demonstrated a wider distribution of liquid velocity inside the reactor volume with comparatively smaller low velocity zones below 0.01 m/s. In addition, a better liquid recirculation was noticed in 1.2 m/s case compared to the 0.6 m/s case.

Even though a considerable amount of biogas has been produced during the operation of the reactor, the simulation results with a source term displayed that the gas generation does not affect the liquid flow fields in a significant manner. But the biogas velocity profiles showed a noticeable change after addition of the source term.

Change of the liquid distribution arrangement resulted in some interesting changes to gas and liquid flow characteristic of the reactor. 15 minutes of alternative gas distribution pattern was successfully simulated with a 1 minute pause after each stage. The results indicated that a similar flow pattern of gas and liquid when the gas distribution system switches between two sides. The liquid velocities were comparatively higher at the top section of the tank in contrast to the other simulation cases. The liquid velocity contours displayed a bulk motion of liquid towards the gas inlet with less significant liquid recirculation zones. But the initial gas distribution arrangement demonstrated better liquid mixing characteristics with four significant recirculation zones. Therefore, it can be concluded from the simulation results that a better mixing performances in the biogas reactor may be achieved by employing initial 10 pipe gas distribution arrangement.

8.1 Recommendations for Future Work

This study was mainly carried out as an initial phase of a research project between VEAS and Telemark University College. The literature review carried out during this study has revealed that there are numerous parameters affecting the flow fields and reactor performances. Due to the time constraints, this study has only focused on few parameters such as bubble size, inlet gas velocity, biogas generation and gas distribution arrangement.

Location of the gas inlet can influence the flow fields and liquid recirculation in a significant way. The results in this study showed the development of some low velocity zones especially at the bottom part of the tank and at the center of the tank. Therefore, it is recommended to change the distance of the gas inlet from the bottom of the tank and change the radius of the gas distribution system (i.e. distance from wall to the pipes) to compare the results with this case.

Number of pipes and the diameter of the pipes can also be varied to check the variation of the flow characteristics inside the tank. Both of these parameters directly affect the inlet gas velocity as long as the volumetric gas flow rate keeps as constant.

Gas distribution arrangement will also play a major role in maintaining proper liquid recirculation inside the reactor. According to the previous discussion, it can be recommended to use the initial gas distribution arrangement (10 pipes arrangement) which has been used during this project, instead of the existing system at VEAS, as it demonstrated better liquid recirculation characteristics. Most importantly, this change may not need any major modifications to the reactor. Apart from the two gas distribution arrangements used during this study, other gas distribution arrangements can also be employed to compare the flow behavior. For example, 5 alternative pipes can be used at a time to distribute gas instead of using 5 neighboring pipes.

As described in a previous chapter, gas distribution system at VEAS works in 15 minutes intervals with a pause of 5-10 minutes. Optimization of this time intervals is essential to

achieve a better mixing throughout the AD process. It is recommended to simulate the process with different time intervals in order to identify the optimum gas distribution sequence.

Even though all the simulations in this study have run with single characteristic bubble size to reduce the computational effort, it is recommended to simulate the process with at least 2 or 3 bubble sizes treating as different secondary phases. This will in fact provide a better representation of the gas phase which is having a bubble size distribution rather than a single bubble size. But this will probably require an upgrade to the existing workstations preferably with high speed computers equipped with increased system memory and parallel processing capabilities.

It is common for most of the CFD simulation studies in the literature to validate the model with experimental results. Studies carried out by Degalesan *et al*. demonstrate the possibility of using computer automated radioactive particle tracking (CARPT) method to investigate the liquid recirculation and turbulence in bubble columns[22]. Therefore, it can be recommended to obtain experimental results of the flow fields in the biogas reactor using such a method and compare them with the simulation results.

References

[1] Wikipedia The Free Encyclopedia. (2013). *Pollution*. Available: http://en.wikipedia.org/wiki/Environmental_pollution

[2] Wikipedia The Free Encyclopedia. (2013). *Water Pollution*. Available: http://en.wikipedia.org/wiki/Water_pollution

[3] Wikipedia The Free Encyclopedia. (2013). *Sewage Treatment*. Available: http://en.wikipedia.org/wiki/Sewage_treatment

[4] S. Latha, D. Borman, and P. Sleigh, "CFD multiphase modelling for evaluation of gas mixing in an anaerobic digester," 2009.

[5] P. Sagberg, P. Ryrfors, and K. Berg, "Years of Operation of an Integrated Nutrient Removal Treatment Plant: Ups and Downs. Part 2: Sludge and Side Stream Treatment," *VEAS*.

[6] *VEAS Official Website*. Available: http://www.veas.nu/

[7] P. J. Jørgensen, *Biogas-Green Energy: Process, Design, Energy Supply, Environment*: Researcher for a Day, 2009.

[8] Friends of the Earth. (2007, Briefing Anaerobic digestion. Available: http://www.foe.co.uk/resource/briefings/anaerobic_digestion.pdf

[9] T. Al Seadi, *Biogas handbook*: Syddansk Universitet, 2008.

[10] Wikipedia The Free Encyclopedia. (2013). *Anaerobic digestion*. Available: http://en.wikipedia.org/wiki/Anaerobic_digestion

[11] M. Terashima, R. Goel, K. Komatsu, H. Yasui, H. Takahashi, Y. Li, *et al.*, "CFD simulation of mixing in anaerobic digesters," *Bioresource technology*, vol. 100, pp. 2228-2233, 2009.

[12] A. Akhtar, M. O. Tade, and V. K. Pareek, "Two-fluid eulerian simulation of bubble column reactors with distributors," *Journal of chemical engineering of Japan*, vol. 39, pp. 831-841, 2006.

[13] D. Law, "Computational Modeling And Simulations Of Hydrodyanmics For Air-Water External Loop Airlift Reactors," Virginia Polytechnic Institute and State University, 2010.

[14] D. Zhang, *Eulerian modeling of reactive gas-liquid flow in a bubble column*: University of Twente, 2007.

[15] V. V. Buwa, D. S. Deo, and V. V. Ranade, "Eulerian–Lagrangian simulations of unsteady gas–liquid flows in bubble columns," *International journal of multiphase flow*, vol. 32, pp. 864-885, 2006.

[16] V. V. Buwa and V. V. Ranade, "Mixing in bubble column reactors: role of unsteady flow structures," *The Canadian Journal of Chemical Engineering*, vol. 81, pp. 402-411, 2003.

[17] A. Hekmat, A. E. Amooghin, and M. K. Moraveji, "CFD simulation of gas–liquid flow behaviour in an air-lift reactor: determination of the optimum distance of the draft tube," *Simulation Modelling Practice and Theory*, vol. 18, pp. 927-945, 2010.

[18] T. J. Casey. (2009, DIFFUSED AIR AERATION SYSTEMS FOR THE ACTIVATED SLUDGE PROCESS - DESIGN PERFORMANCE TESTING. Available: http://www.aquavarra.ie/AerationP4.pdf

[19] Berdal Strømme, "SLAMSTABILISERINGSANLEGG TEGNINGER," VEAS1996.

[20] ANSYS Inc., "ANSYS FLUENT 12.0/12.1 Theory Guide," 2009.

[21] X. Wang, J. Ding, N.-Q. Ren, B.-F. Liu, and W.-Q. Guo, "CFD simulation of an expanded granular sludge bed (EGSB) reactor for biohydrogen production," *International Journal of Hydrogen Energy*, vol. 34, pp. 9686-9695, 2009.

[22] S. Degaleesan, M. Dudukovic, and Y. Pan, "Experimental study of gas-induced liquid-flow structures in bubble columns," *AIChE Journal*, vol. 47, pp. 1913-1931, 2001.

[23] R. Zevenhoven and P. Kilpinen, *Control of pollutants in flue gases and fuel gases*: Helsinki University of Technology, 2001.

[24] L. A. Tokheim, "Gas Purification," Lecture Notes - Spring 2012 ed.

Appendix A: Project Task Description

Telemark University College

Faculty of Technology

FMH606 Master's Thesis

Title: Simulation of gas and liquid flow in biogas reactor using Fluent

TUC supervisor: Knut Vågsæther

External partner: VEAS

Task description:

- Make a literature review on bio gas reactors and gas-liquid flow in tanks.
- Make computational mesh of one of the bio gas reactors at VEAS.
- Simulate the flow of gas and liquid in the reactor tank with Fluent.
- Investigate how the boundary conditions (gas bubble size, velocity etc.) influence the flow field.
- Analyze data and discuss the behavior of the flow field
- If possible: recommend changes in operation and justify these recommendations with simulations.
- Write report.

Task background:

VEAS (veas.nu) is a sewage treatment plant located in Røyken at the Oslo-fjord. It serves over 500 000 people in Oslo and Akershus.

The four bio-gas reactors at VEAS are each 6000 m3 and made of concrete. The circulation in the tank is achieved by pumping bio gas from the top of the tank down to the bottom. It is very difficult to measure the flow field in the tank and simulations are required to get a understanding of how the flow of gas and liquid behaves in the reactors.

Student category:

PT and EET (CFD course)

Address: Kjølnes ring 56, NO-3918 Porsgrunn, Norway. **Phone:** 35 57 50 00. **Fax:** 35 55 75 47.

Practical arrangements:

The student will work at TUC but a few visits to the VEAS plant is needed.

Signatures:

Student:	Sithara Dayarathna	2013-02-04
Supervisor:	Knut Vågsæther	2013-02-04

Appendix B: Calculation of Inlet Gas Velocity

Operational conditions at VEAS biogas reactor;

Volumetric flow rate of gas = 300 Nm3/h

Pressure of the inlet gas = 200000 Pa

Temperature of the inlet gas = 67 ^{o}C (340 K)

Normal Conditions;

Pressure at the normal conditions = 101325 Pa

Temperature at the normal conditions = 273.15 K

Assuming ideal gas law,

$$PV = nRT \qquad \text{B-1}$$

Where,

P = Pressure of the gas [Pa]

V = Volumetric flow rate of the gas [m^3/h]

n = Number of moles of the gas [mol]

R = Universal gas constant [J/mol.K]

T = Temperature of the gas [K]

Substituting the normal and actual conditions of the gas in the Equation B-1 and dividing each other will calculate the actual volumetric flow of gas as,

$$\frac{101325 * 300}{200000 * \dot{V}} = \frac{nR * 273.15}{nR * 340}$$

Actual volumetric gas flow rate from 1 pipe = 189.18/10 = 18.92 m^3/h

Substituting volumetric flow of the gas and cross sectional area of a pipe in following equation,

$$\dot{V} = A * v \qquad \text{B-2}$$

Where,

V = Volumetric flow rate of gas (m3/h)

A= Cross sectional area of the pipe (m)

v = Gas velocity through the pipe (m/s)

Inlet gas velocity = 1.189 m/s ~ 1.2 m/s

Appendix C: Calculation of the Source Term

Source term is defined as the rate of generation of gas per unit volume liquid inside the reactor.

Rate of generation of gas = 320 Nm^3/h (Data from VEAS)

Molecular weight of gas = 28.996*10-3 (kg/mol) (as the air has been used instead of biogas)

Volume of the tank = 5773.7 m^3 (from FLUENT mesh details)

Substituting the normal conditions in the ideal gas equation,

$$\frac{101325 * 320}{3600} = \frac{\dot{m} * 8.314 * 273.15}{28.996 * 10^{-3}}$$

Rate of generation of gas = 0.1148 kg/s

Source term can be calculated as;

$$Source\ term = \frac{\dot{m}}{V_{tank}}$$

Source term = 1.9896*10-5 ~ $2*10^{-5}$ $kg/m^3.s$

Appendix D: Calculation of Terminal Velocity of a Gas Bubble

Forces acting on a gas bubble inside a liquid are illustrated in the Figure D- 1.

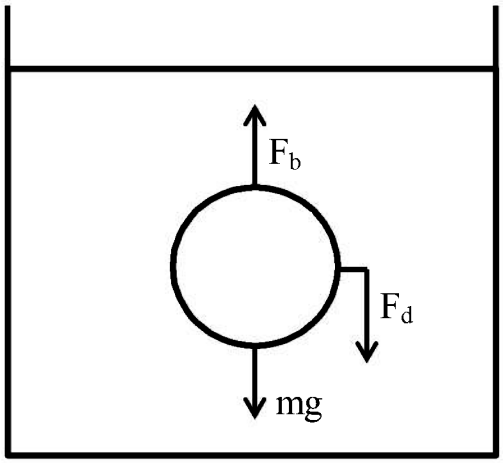

Figure D- 1: Forces acting on a gas bubble inside a liquid.

Fb – Buoyancy force exerted from the liquid on the bubble

Fd – Drag (friction) force on the bubble against its motion

mg – Gravitational force on the bubble due to its mass

When the above forces exerted on the bubble level off with each other, it reach into an equilibrium state with a constant velocity which is referred as terminal velocity[23]. The terminal velocity of a gas bubble in a liquid can be expressed as,

$$V_t = \sqrt{\frac{(\rho_{fluid} - \rho_{gas})}{\rho_{fluid}} \frac{4g * D_p}{3C_D}} \qquad \text{D-1}$$

Where,

V_t = Terminal velocity of the bubble [m/s]

ρ_{fluid} = Density of the fluid [kg/m^3]

ρ_{gas} = Density of the gas [kg/m^3]

g = Gravitational acceleration [m/s^2]

D_p = Diameter of the gas bubble [m]

C_D = Drag coefficient [-]

Assuming stokes regime, drag coefficient can be given as

$$C_D = \frac{24}{Re_D} \quad \text{D-2}$$

Where,

Re_D = Droplet Reynolds number [-]

Droplet Reynolds number can be expressed as,

$$Re_D = \frac{\rho_{fluid} * V_t * D_p}{\mu_{fluid}} \quad \text{D-3}$$

Where,

Vt = Terminal velocity of the droplet [m/s]

ρ_{fluid} = Density of the fluid [kg/m^3]

D_p = Diameter of the gas bubble [m]

μ_{fluid} = Viscosity of the fluid [Pa.s]

Substituting Equation D-3 in D-2 and then D-2 in D-1 will provide an equation for terminal velocity for stokes regimes as,

$$V_t = \frac{g D_p^2 (\rho_{fluid} - \rho_{gas})}{18 \mu_{fluid}} \quad \text{D-4}$$

Substituting the following values in the Equation D-4 will calculate an initial value for terminal velocity.

Liquid density = 998.2 kg/m^3 (FLUENT database)

Gas density = 2.55 kg/m^3 (Average velocity of gas phase for a general case)

Liquid viscosity = 0.001 Pa.s

g = 9.81 m/s^2

Bubble diameter = 0.005 m

Terminal velocity of the 5 mm bubble size = 13.52 m/s

Calculated terminal velocity is then used to validate the assumption of stokes regime by substituting in Equation D-3. If the resulting Reynolds number is greater than 1, the settling regime should be treated as turbulent[24].

Preliminary Reynolds number of the 5 mm bubble = 67302

Therefore, the settling regime was taken as turbulent.

For the turbulent settling regimes, Reynolds number is defined as[23],

$$Re_D = 0.1334 * Ar^{0.7016} \quad \text{D-5}$$

Where,

Ar = Archimedes number

Archimedes number is defined as,

$$Ar = \frac{\rho_{fluid}\left(\rho_{fluid} - \rho_{gas}\right) * g * D_p^3}{\mu_{fluid}^2} \quad \text{D-6}$$

After calculating the new Reynolds number from the Equation D-5, the new turbulent velocity can be easily calculated from the Equation D-7.

$$V_t = \frac{Re_D * \mu_{fluid}}{\rho_{fluid} * D_p} \quad \text{D-7}$$

New terminal velocity of the 5 mm bubble size = 0.5 m/s

Time to reach the bubble to the liquid surface = 19.15/ 0.5 = 38.5 s

The terminal velocity and rise to of a range of bubble sizes from 1 mm to 10 mm were calculated and plotted to observe any underlying trends. Calculation results for all the bubble sizes are presented in Table D- 1. Figure D- 2 illustrates the variation of terminal velocity and bubble rise time against bubble diameter.

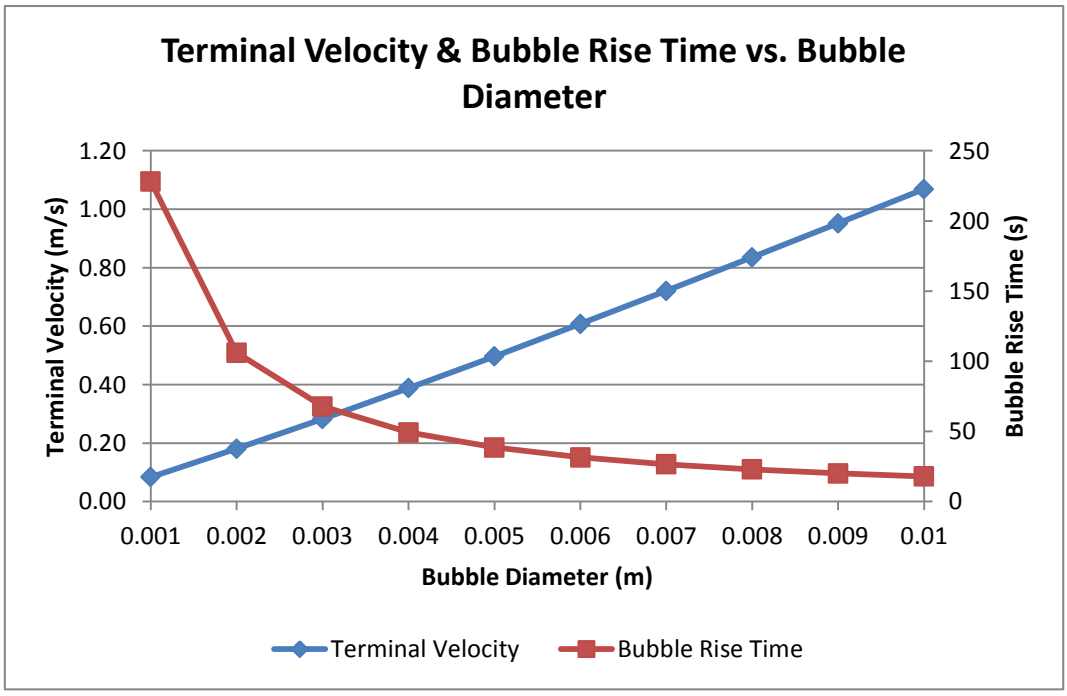

Figure D- 2: Variation of terminal velocity and rise time of a gas bubble with bubble size.

Table D- 1: Calculation results for terminal velocity and rise time of bubble sizes from 1 mm to 10 mm.

Particle Diameter [m]	0.001	0.002	0.003	0.004	0.005	0.006	0.007	0.008	0.009	0.01
Preliminary Terminal Velocity [m/s]	0.5	2.2	4.9	8.7	13.5	19.5	26.5	34.6	43.8	54.1
Preliminary Renolds Number [-]	538	4307	14537	34459	67302	116298	184677	275670	392506	538417
Archimedes Number [-]	9692	77532	261671	620257	1211439	2093366	3324188	4962053	7065110	9691509
New Reynolds Number [-]	84	359	844	1546	2473	3630	5021	6650	8521	10637
New Terminal Velocity [m/s]	0.08	0.18	0.28	0.39	0.50	0.61	0.72	0.84	0.95	1.07
Time to reach the top [s]	228.1	106.0	67.8	49.3	38.5	31.5	26.6	22.9	20.1	17.9

Appendix E: Comparison of Gas Velocity Contours

A comparison of gas velocity profiles for different cases of study is presented below. Snapshots were taken after the flow fields reached to a stable behavior.

Gas Velocity Profiles for Different Bubble Diameters

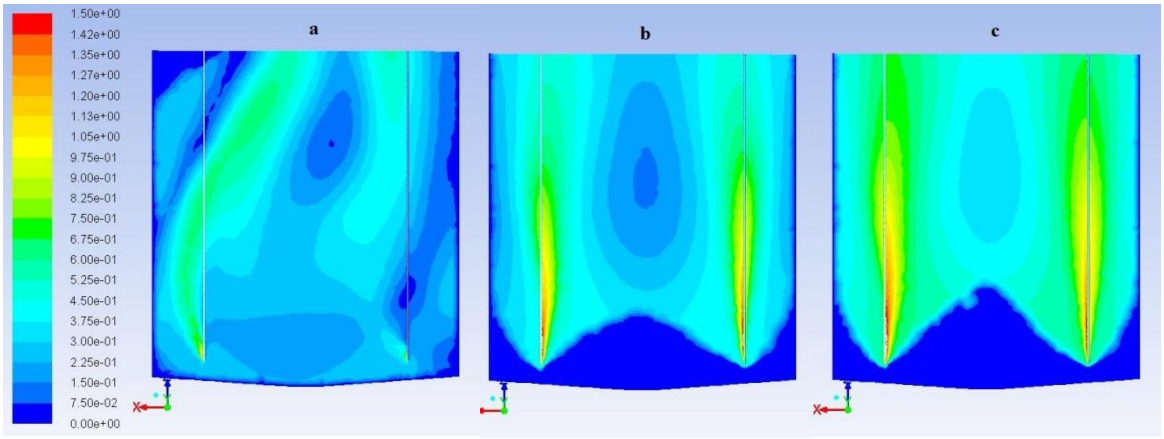

Figure E- 1: Gas velocity profiles of a) 1 mm b) 5 mm c) 10 mm bubble sizes at vertical plane of Y=0.

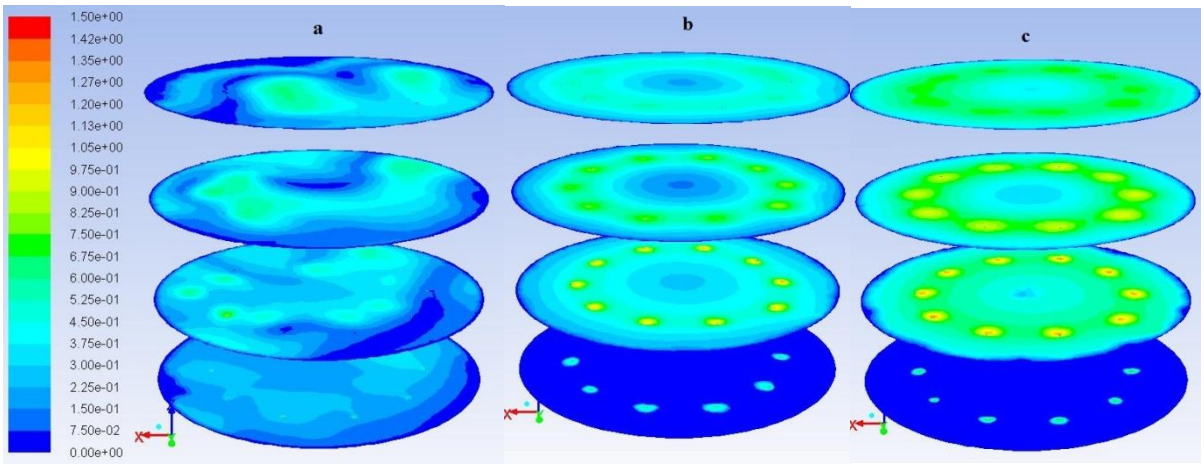

Figure E- 2: Gas velocity profiles of a) 1 mm b) 5 mm c) 10 mm bubble sizes at horizontal planes.

Gas Velocity Profiles for Different Inlet Gas Velocities

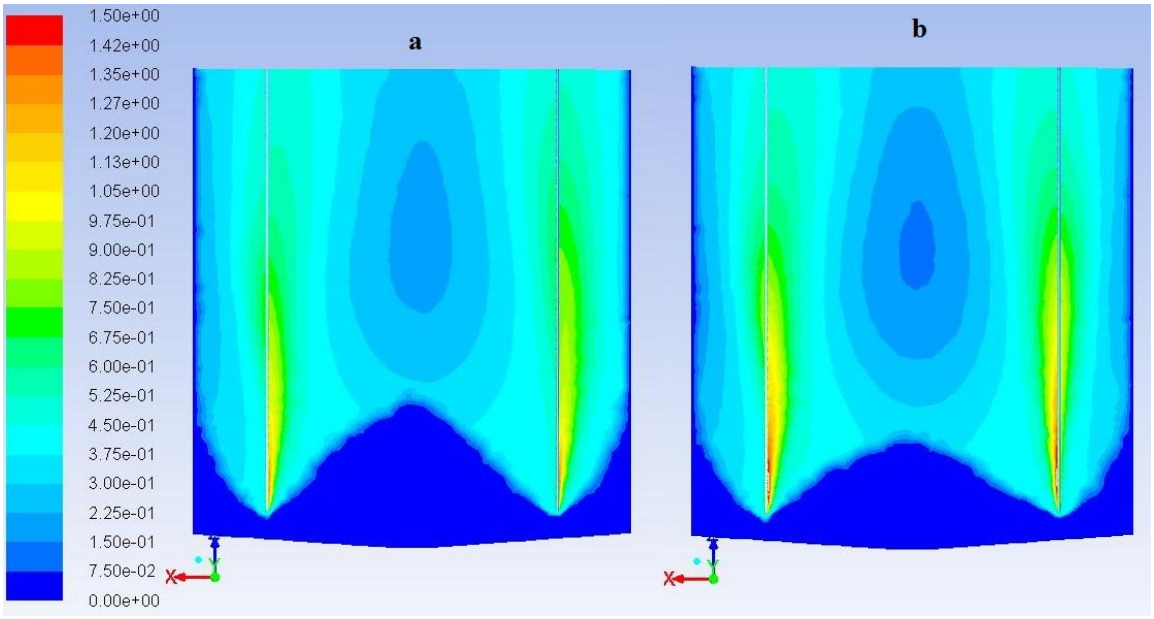

Figure E- 3: Gas velocity profiles of a) 0.6 m/s b) 1.2 m/s inlet gas velocity case at vertical plane Y=0.

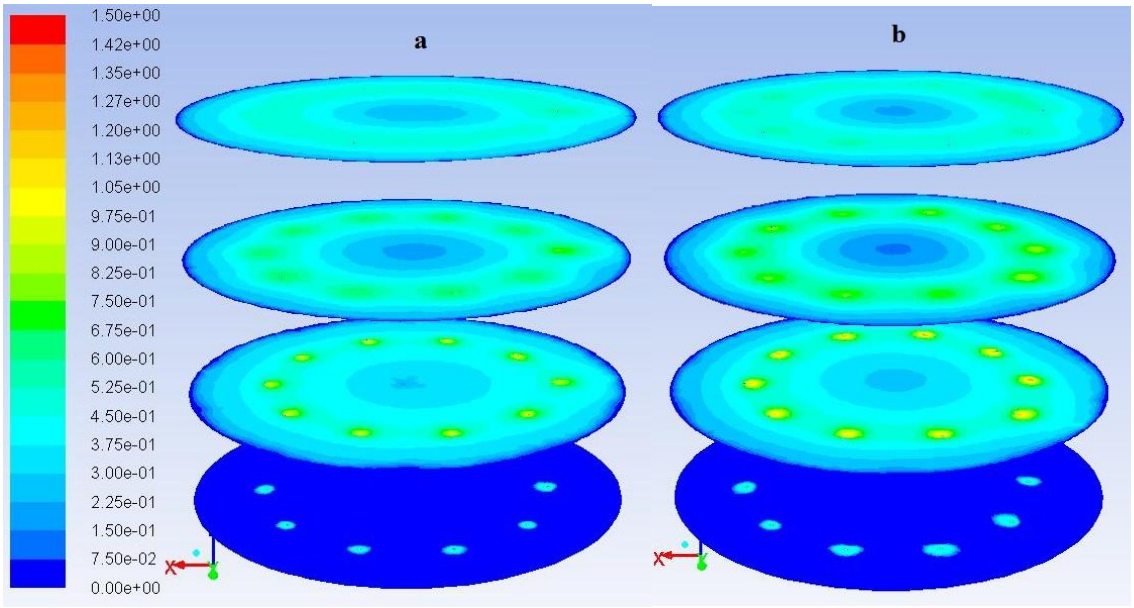

Figure E- 4: Gas velocity profiles of a) 0.6 m/s b) 1.2 m/s inlet gas velocity case at horizontal planes.

Gas Velocity Profiles With and Without Source Term

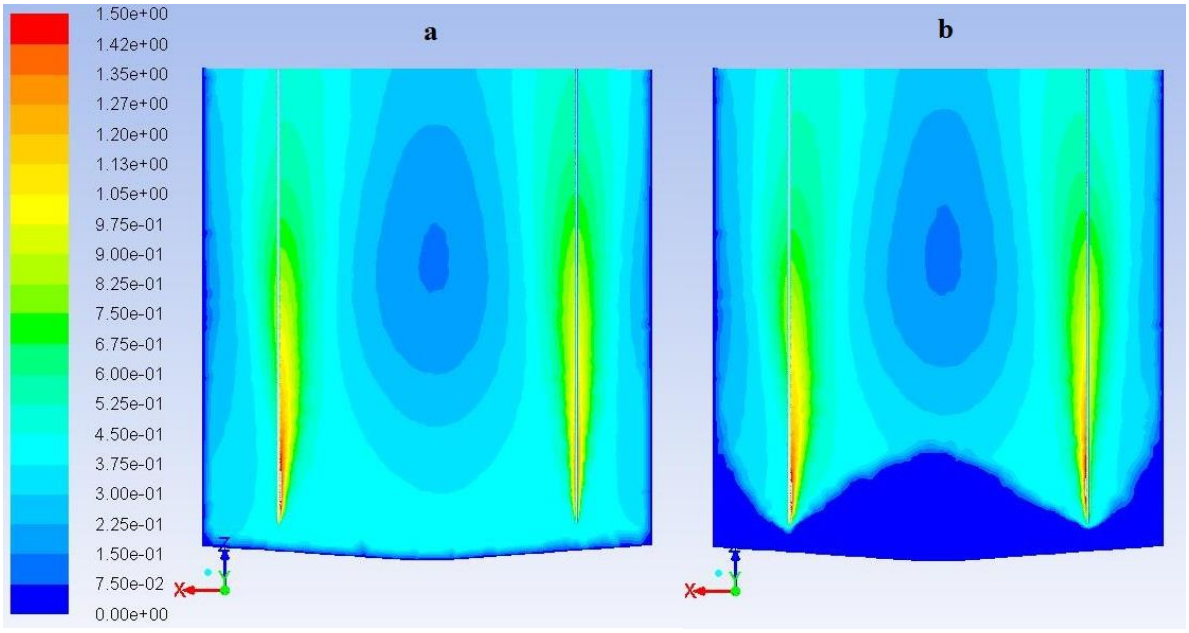

Figure E- 5: Gas velocity profiles a) with b) without source term at vertical plane Y=0.

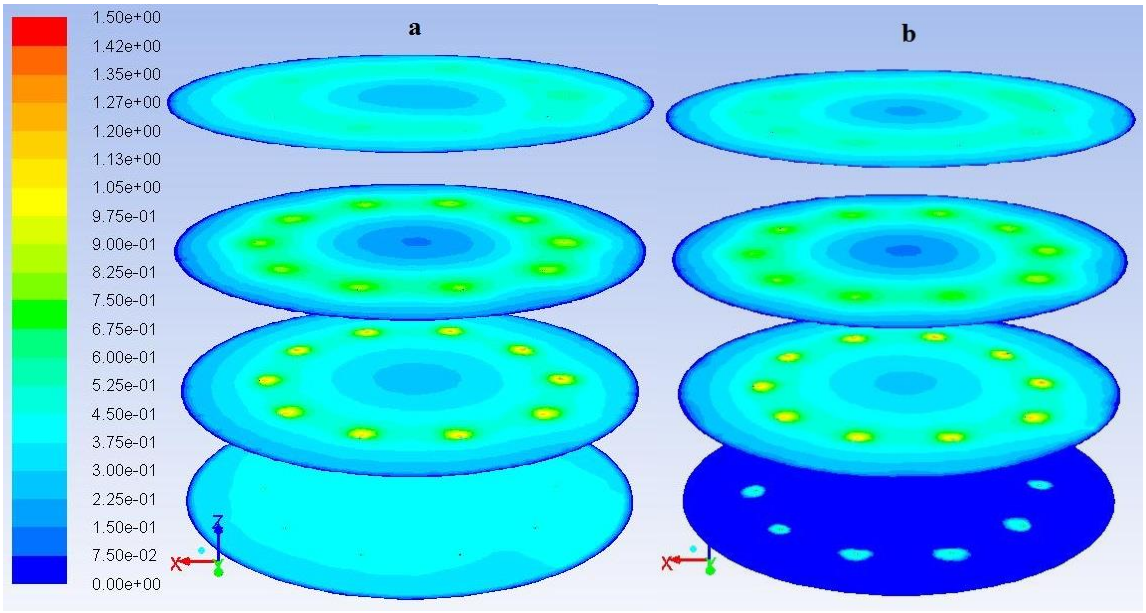

Figure E- 6: Gas velocity profiles a) with b) without source term at horizontal planes.

Gas Velocity Profiles for Different Gas Distribution Systems

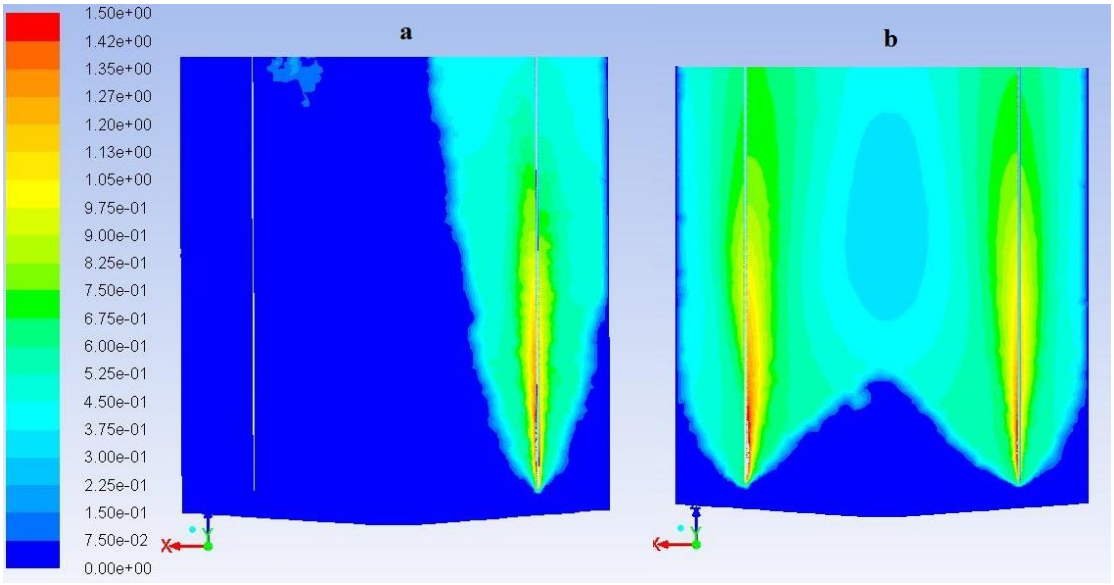

Figure E- 7: Gas velocity profiles of a) two velocity inlet b) one velocity inlet gas distribution system at vertical plane Y=0.

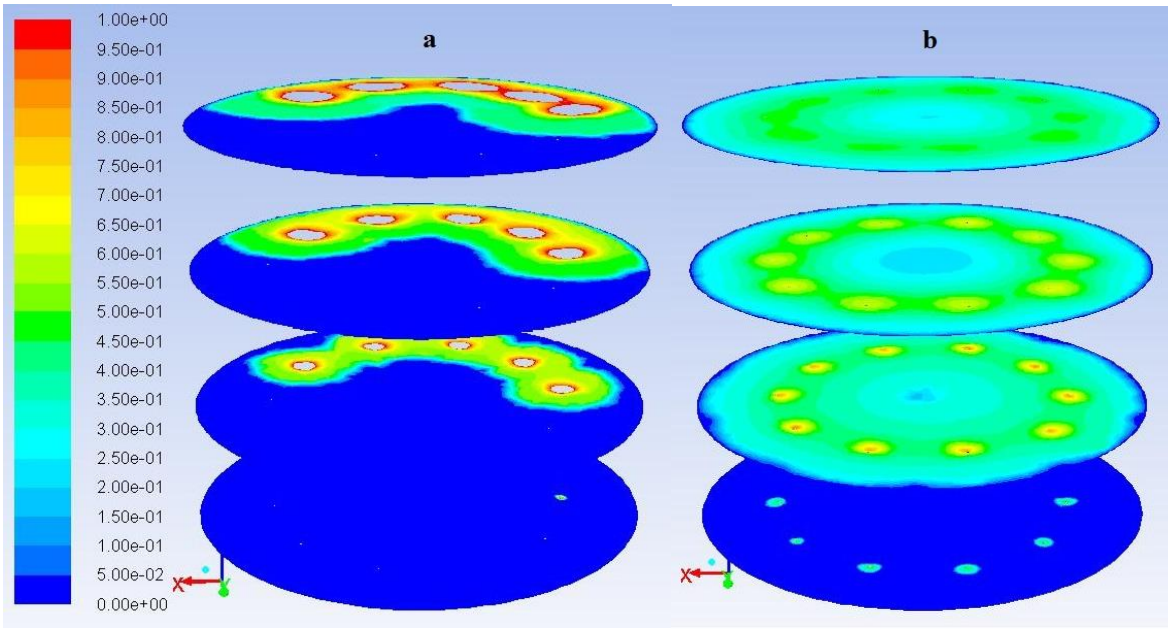

Figure E- 8: Gas velocity profiles of a) two velocity inlet b) one velocity inlet gas distribution system at horizontal planes.

Appendix F: XY Plots of Gas Velocity Distribution

Gas velocity distribution across the diameter of the tank were also obtained at four different liquid levels of Z=1, 6, 12, 18 m for all the cases of study.

Gas Velocity Distribution for Different Bubble Diameters

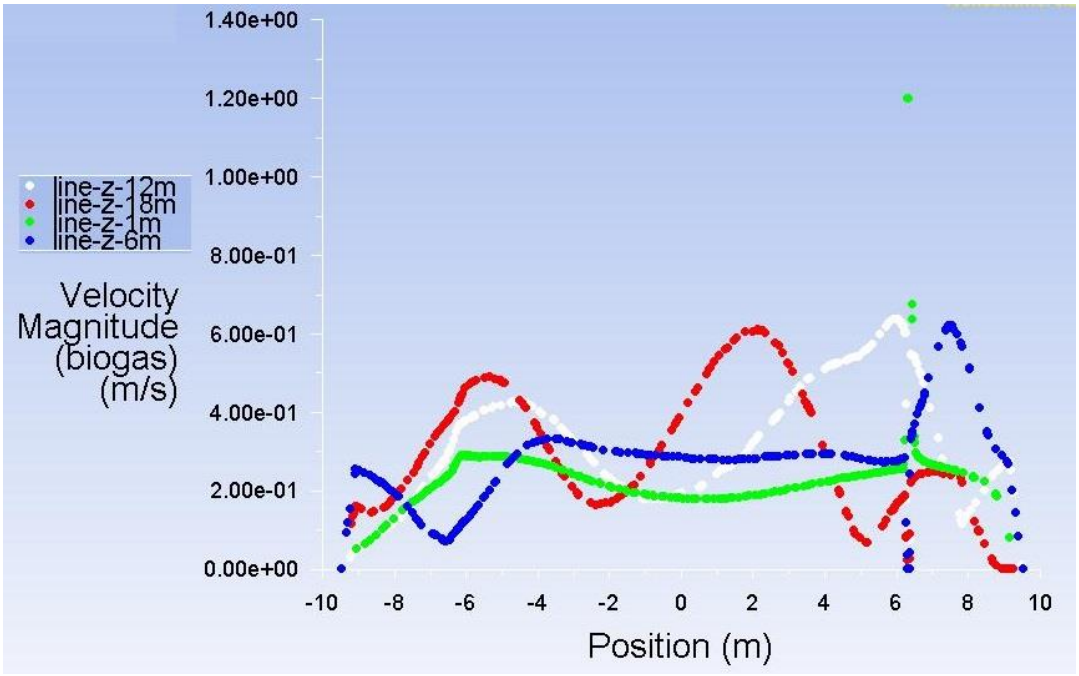

Figure E- 9: Gas velocity distribution across the tank diameter for 1 mm bubble size.

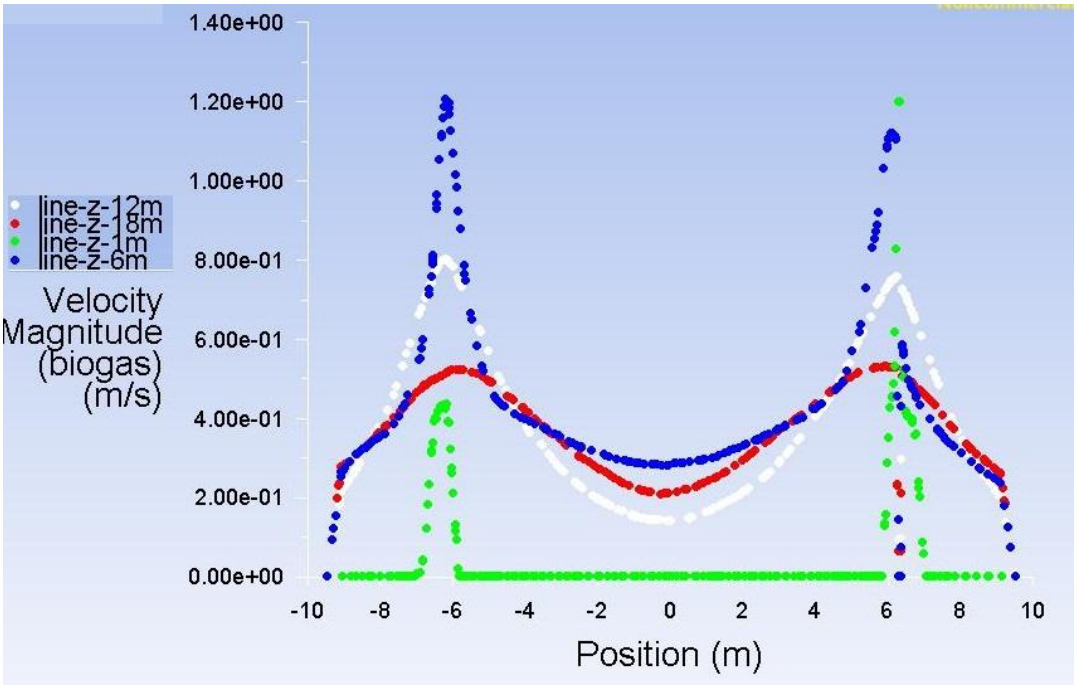

Figure E- 10: Gas velocity distribution across the tank diameter for 5 mm bubble size.

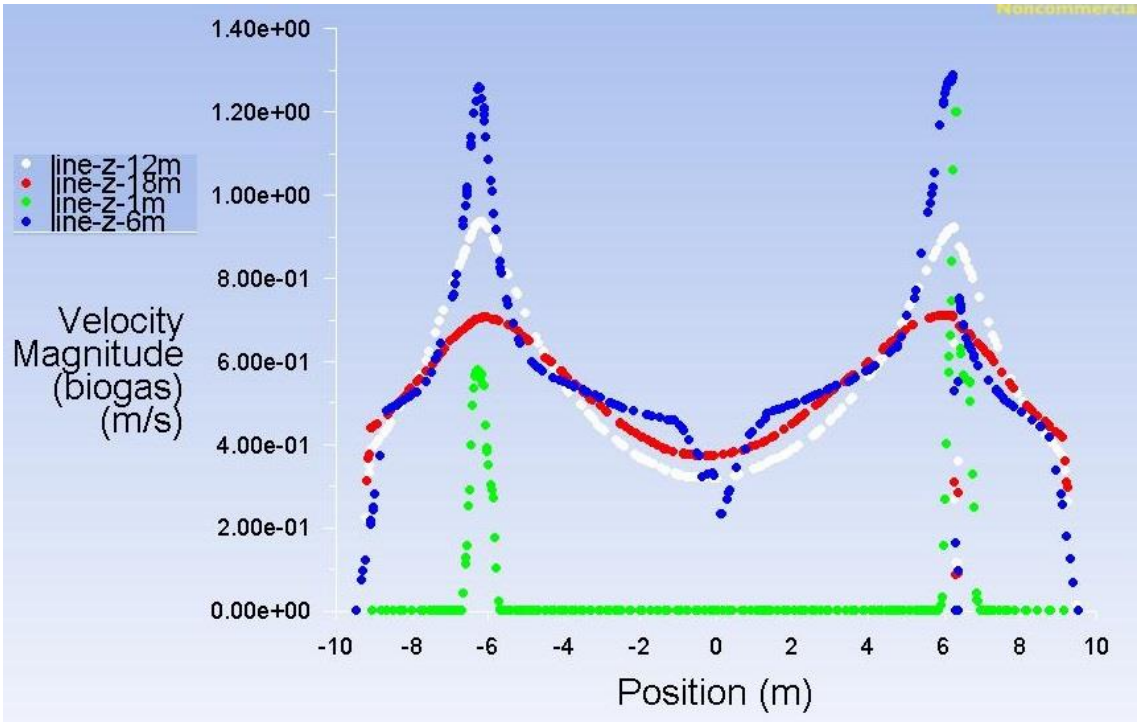

Figure E- 11: Gas velocity distribution across the tank diameter for 10 mm bubble size.

Gas Velocity Distribution for 0.6 m/s Inlet Gas Velocity Case

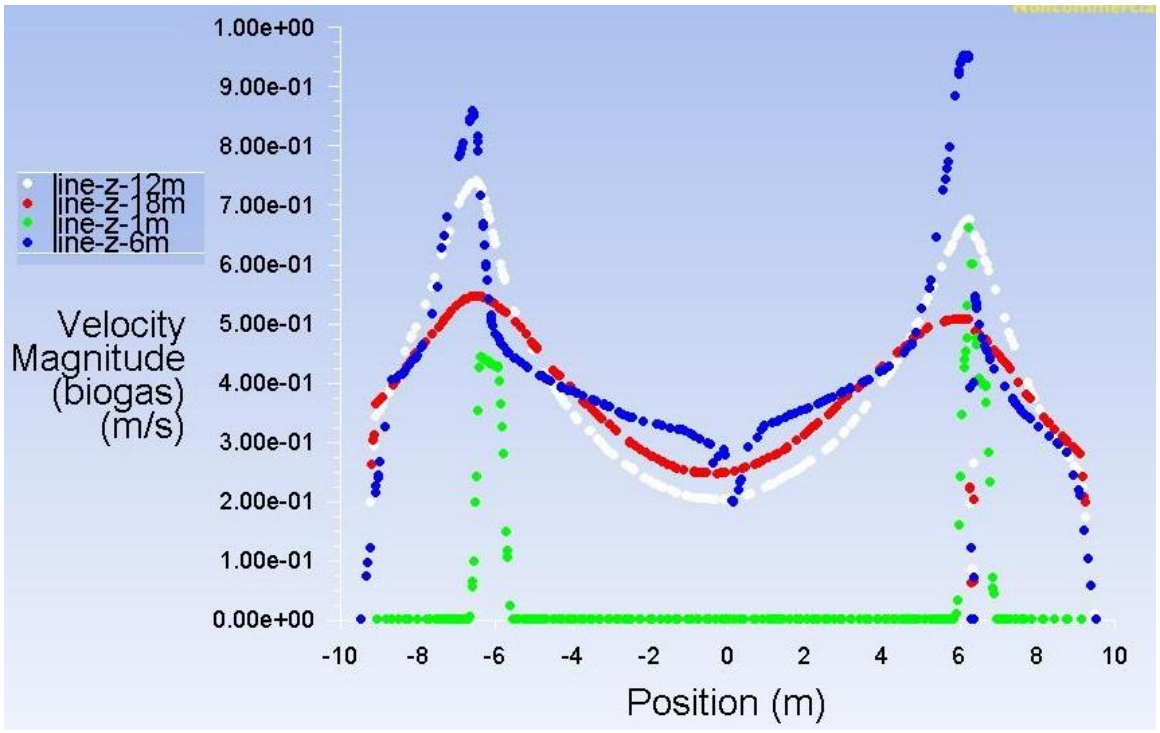

Figure E- 12: Gas velocity distribution across the tank diameter for 0.6 m/s inlet gas velocity.

Gas Velocity Distribution with the Source Term

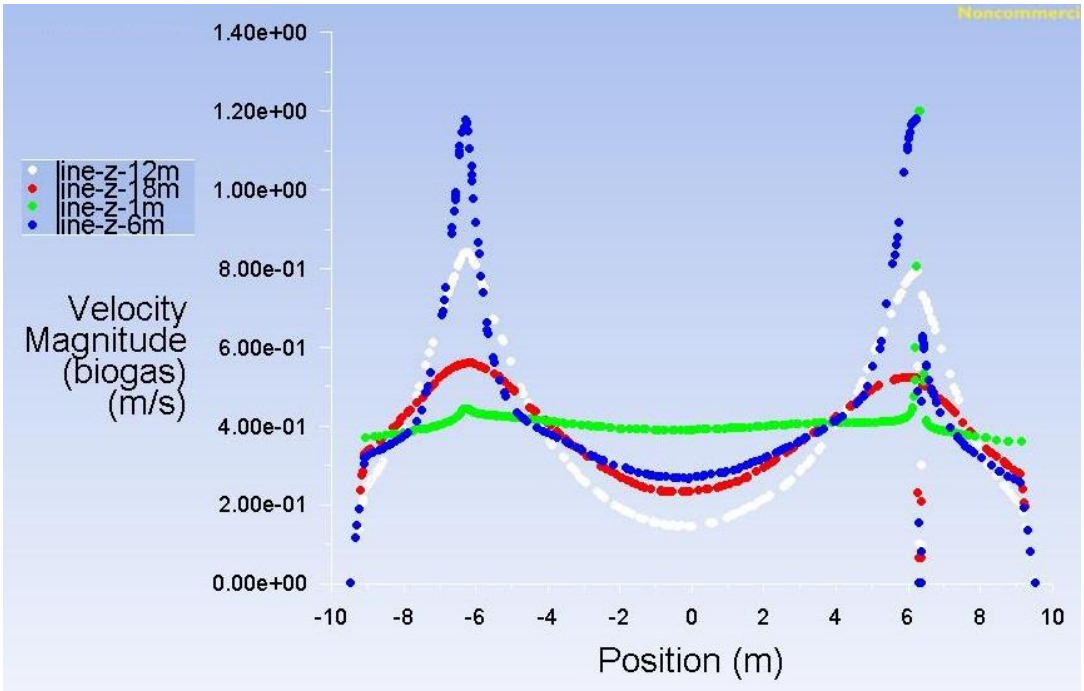

Figure E- 13: Gas velocity distribution across the tank diameter after including source term.

Gas Velocity Distribution for Existing 5 Pipe Gas Distribution Systems

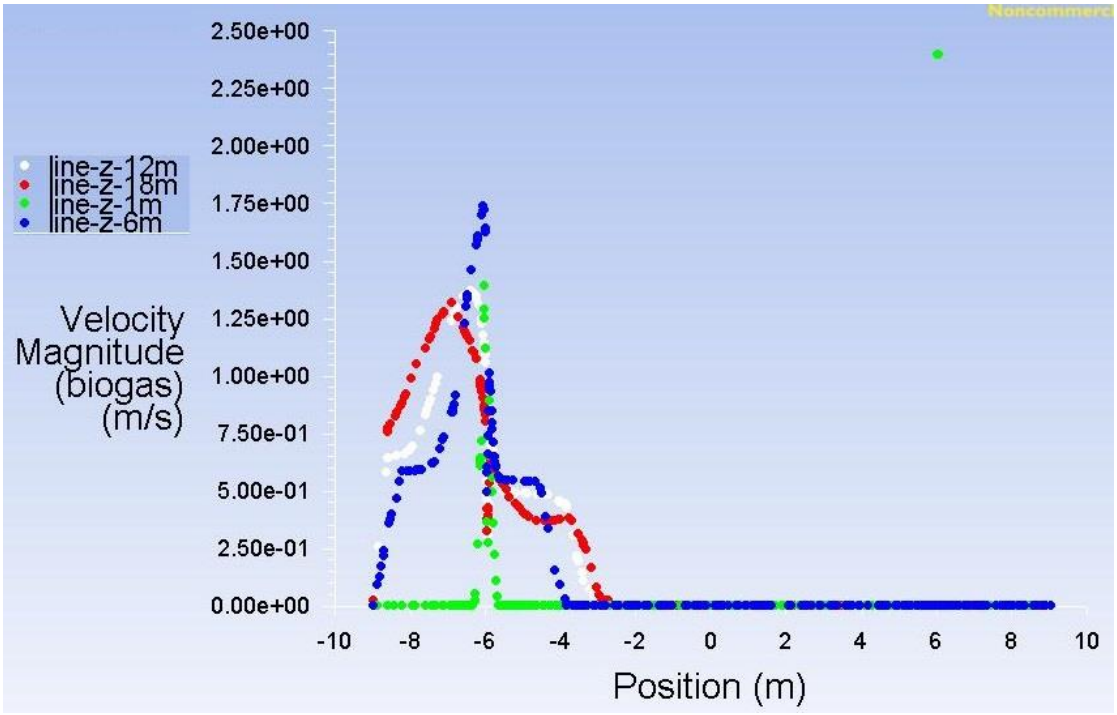

Figure E- 14: Gas velocity distribution across the tank diameter after 900 s for existing 5 pipes gas distribution arrangement.

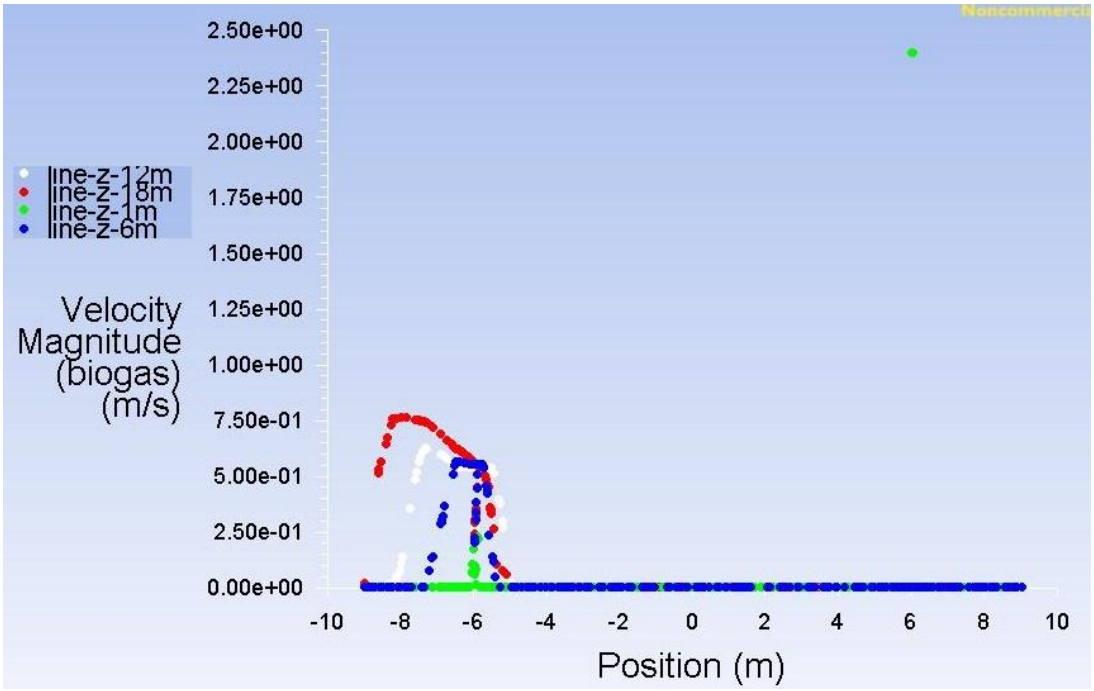

Figure E- 15: Gas velocity distribution across the tank diameter after 960 s for existing 5 pipes gas distribution arrangement.

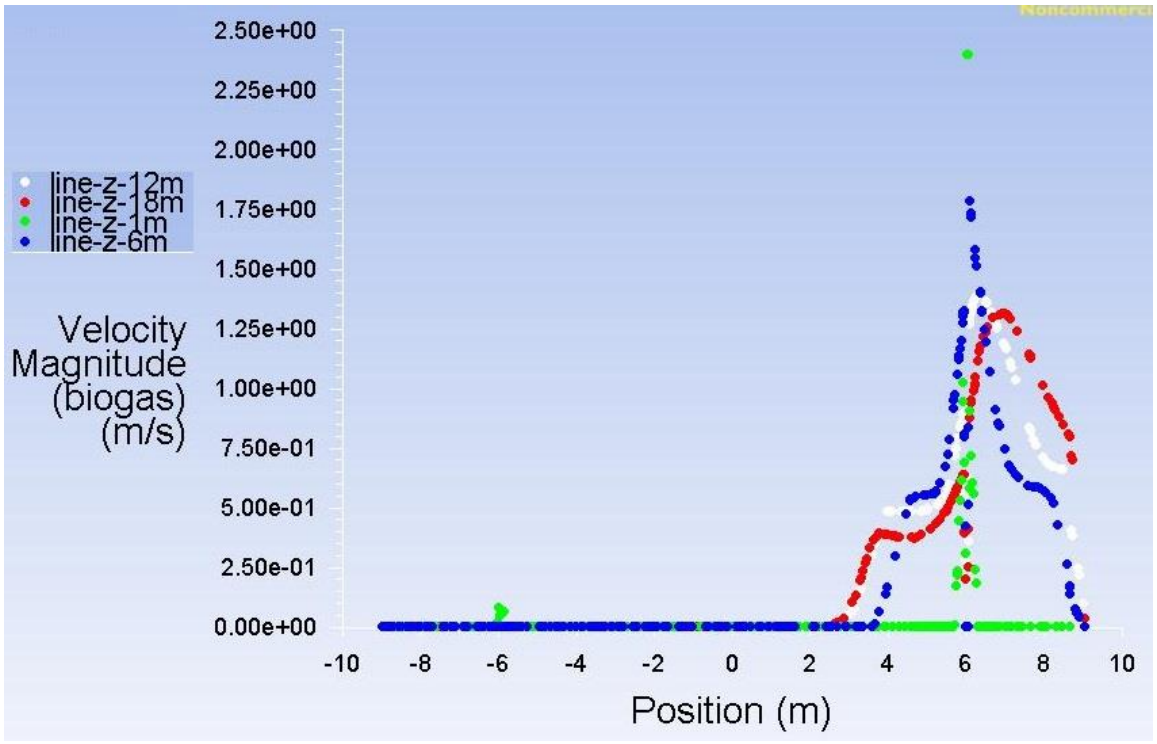

Figure E- 16: Gas velocity distribution across the tank diameter after 1860 s for existing 5 pipes gas distribution arrangement.